Effects of nuclear factor I phosphorylation on calpastatin (*CAST*) gene variant expression and subcellular distribution in malignant glioma cells

Received for publication, July 7, 2018, and in revised form, November 29, 2018 Published, Papers in Press, November 30, 2018, DOI 10.1074/jbc.RA118.004787

The Minh Vo, Rebecca Burchett, Miranda Brun, Elizabeth A. Monckton, Ho-Yin Poon, and Roseline Godbout[1]

From the Department of Oncology, University of Alberta, Cross Cancer Institute, Edmonton, Alberta T6G 1Z2, Canada

Edited by Xiao-Fan Wang

Malignant glioma (MG) is the most lethal primary brain tumor. In addition to having inherent resistance to radiation treatment and chemotherapy, MG cells are highly infiltrative, rendering focal therapies ineffective. Genes involved in MG cell migration and glial cell differentiation are up-regulated by hypophosphorylated nuclear factor I (NFI), which is dephosphorylated by the phosphatase calcineurin in MG cells. Calcineurin is cleaved and thereby activated by calpain proteases, which are, in turn, inhibited by calpastatin (CAST). Here, we show that the *CAST* gene is a target of NFI and has NFI-binding sites in its intron 3 region. We also found that NFI-mediated regulation of *CAST* depends on NFI's phosphorylation state. We noted that occupation of *CAST* intron 3 by hypophosphorylated NFI results in increased activation of an alternative promoter. This activation resulted in higher levels of *CAST* transcript variants, leading to increased levels of CAST protein that lacks the N-terminal XL domain. CAST was primarily present in the cytoplasm of NFI-hypophosphorylated MG cells, with a predominantly perinuclear immunostaining pattern. NFI knockdown in NFI-hypophosphorylated MG cells increased CAST levels at the plasma membrane. These results suggest that NFI plays an integral role in the regulation of *CAST* variants and CAST subcellular distribution. Along with the previous findings indicating that NFI activity is regulated by calcineurin, these results provide a foundation for further investigations into the possibility of regulatory cross-talk between NFI and the CAST/calpain/calcineurin signaling pathway in MG cells.

Malignant glioma (MG),[2] encompassing World Health Organization grade III (anaplastic astrocytoma) and IV (glioblastoma) astrocytomas, is the most common and deadly form of adult primary brain tumor (1). Despite aggressive treatment by surgical resection, radiation therapy, and adjuvant chemotherapy, patient prognosis remains dismal, with a median survival time of less than 5 years for anaplastic astrocytoma and 15 months for glioblastoma (2, 3). Tumor recurrence and inevitable treatment failure are, at least in part, due to the highly infiltrative nature of MG cells (4, 5). Post-mortem examination often reveals the dissemination of tumor cells into normal brain parenchyma, frequently found distal from the original tumor mass and at early stages of the disease (6). Early infiltration of tumor cells, together with the inherent resistance of MG cells to cytotoxic drugs and radiation therapy, severely limits the efficacy of conventional focal and systemic treatments (7–9). Whereas targeting infiltrative MG cells would likely be of clinical benefit, molecular mechanisms underlying MG cell migration and infiltration remain poorly characterized.

Our laboratory has previously shown that the expression of brain fatty acid–binding protein (FABP7, B-FABP) is associated with increased MG cell migration *in vitro* (10). FABP7 is found at sites of infiltration in glioblastoma tumors, with elevated levels of FABP7 correlating with decreased survival in glioblastoma patients (11–13). *FABP7* expression is regulated by nuclear factor I (NFI), a family of four transcription factors (NFIA, NFIB, NFIC, and NFIX) (14, 15). NFIs bind to the consensus recognition sequence, 5′-TTGGCN$_{3-6}$GCCAA-3′, as either homodimers or heterodimers through their highly conserved N-terminal DNA-binding domains (16, 17). NFIs can also interact with half of the consensus palindrome sequence, albeit at reduced affinity (18). The variable C-terminal transactivation domain of NFI can either inhibit or activate its target genes, depending on tissue and promoter context (19), with different NFIs able to elicit distinct effects on the same promoter (14). In addition to *FABP7*, a neural progenitor/stem cell marker, NFI regulates genes involved in glial cell differentiation, such as the glial fibrillary acidic protein (*GFAP*) gene (14, 19, 20).

NFI is differentially phosphorylated in MG cells, with the hypophosphorylated form of NFI correlating with *FABP7* and *GFAP* expression (15). Dephosphorylation of NFI is mediated by calcineurin, a calcium-dependent serine/threonine phosphatase (21). Calcineurin, in turn, is cleaved and activated by calpain, a family of calcium-dependent nonlysosomal cysteine proteases (22, 23). The best characterized mechanism for controlling calpain activity is through its endogenous inhibitor, calpastatin, which is encoded by a single gene, *CAST* (24). Calpastatin has a complex expression

This work was supported by Canadian Institutes of Health Research Grant 130314. The authors declare that they have no conflicts of interest with the contents of this article.

This article contains Figs. S1–S4.

[1] To whom correspondence should be addressed: Dept. of Oncology, University of Alberta, Cross Cancer Institute, 11560 University Ave., Edmonton, Alberta T6G 1Z2, Canada. Tel.: 780-432-8901; Fax: 780-432-8892; E-mail: rgodbout@ualberta.ca.

[2] The abbreviations used are: MG, malignant glioma; NFI, nuclear factor I; FABP7, brain fatty acid-binding protein; NE, nuclear extract; 5′-RLM RACE, 5′-RNA ligase-mediated rapid amplification of cDNA ends; CP, canonical promoter; ALT, alternative promoter; CAST, calpastatin; HA, hemagglutinin; qPCR, quantitative PCR; Pol II, polymerase II; CSA, cyclosporin A; GAPDH, glyceraldehyde-3-phosphate dehydrogenase.

profile, both at the RNA and protein levels, a consequence of multiple promoters and alternative splicing (25–27). Based on sequence and structure analyses, full-length murine and bovine calpastatins have four repetitive calpain-inhibitory domains (I–IV) with each domain able to bind to one calpain molecule (28). The function(s) of two extension regions at the N terminus of the calpastatin polypeptide, domains XL (encoded by different combinations of exons $1x_a$, $1x_b$, 1y, and 1z) and L (encoded by exons 2–8), remains poorly understood (25, 29). Four different types of calpastatin have been identified to date based on which domains they contain (30). Three major *CAST* RNA variants have been identified by Northern blot analysis in bovine heart, including two that encode XL-containing and XL-less calpastatin isoforms (25).

Direct binding is required for calpastatin inhibition of calpain activity, with sequestration of calpastatin away from calpain postulated to control local calpain activity (31). Similar to calpain, calpastatin is often found at the plasma membrane and surrounding the nucleus (32). Aggregation of calpastatin in the perinuclear region of the cell may be a mechanism to prevent calpastatin binding to calpain at the plasma membrane (33). In contrast, calpastatin localization at the plasma membrane is believed to inhibit calpain activity through direct binding of calpastatin to calpain. As many known targets of calpain involved in cell migration are found at the plasma membrane, a consequence of calpastatin localization to the plasma membrane may be decreased cell migration (34). Whereas nuclear localization of calpastatin has also been described, its significance remains unclear (35).

ChIP-on-chip experiments to identify targets of NFI in MG cells revealed *CAST* as a putative NFI target gene. Our data indicate that NFI binds to an alternative promoter located upstream of *CAST* exon 4 and affects the relative levels of *CAST* variants transcribed from the canonical *versus* alternative promoters. We show that binding of hypophosphorylated NFI to *CAST* intron 3 results in (i) increased transcriptional activity of *CAST* alternative promoter, (ii) a higher ratio of XL-less to XL-containing *CAST* transcript variants, (iii) loss of calpastatin at the plasma membrane, and (iv) accumulation of calpastatin in the perinuclear region. These findings suggest a key role for NFI in the transcriptional regulation of different *CAST* variants, with accompanying effects on the subcellular distribution of calpastatin.

Results

In vitro occupancy of putative CAST NFI-binding sites

All four NFIs are expressed in cells of glial origin as well as glioblastoma cells, with a number of NFI targets identified in these glial-like cell types (14, 15, 19). An antibody that recognizes all four NFIs was used to identify additional NFI targets in MG cells (36). Analysis of ChIP-on-chip data obtained with this pan-specific NFI antibody and FABP7/GFAP-expressing U251 MG cells resulted in the identification of *CAST* as a putative target of NFI (36). Sequence analysis of DNA bound by NFI revealed three putative NFI recognition sites located within the intronic region upstream of exon 4: C1 (−3928 to −3915 bp), C2 (−3663 to −3628 bp), and C3 (−3469 to −3453 bp) with +1 defined as the first nucleotide of exon 4 (Fig. 1, *A* and *B*). To verify protein binding to these three putative NFI recognition sites, we performed gel shift assays with nuclear extracts prepared from U87 and U251 MG cells. C1, C2, and C3 double-stranded oligonucleotides radiolabeled with [α-^{32}P]dCTP were incubated with (+) or without (−) nuclear extracts and separated on native polyacrylamide gels. Although protein–DNA complexes were detected with all three probes, the shifted bands observed with C1 were considerably weaker than those observed with C2 and C3 probes (see Fig. 2*A* for U87 results). Weak binding to C1 is likely due to poor conservation of the first palindromic half of the NFI consensus sequence, with one of the two conserved guanine residues missing from this site (Fig. 1*B*). We therefore focused on the C2 and C3 NFI recognition sites in subsequent experiments.

Protein binding to the C2 and C3 oligonucleotides was examined using nuclear extracts prepared from both NFI-hyperphosphorylated U87 and NFI-hypophosphorylated U251 MG cells (14, 15). These cell lines express all four NFIs, with similar amounts of *NFIA* RNA and higher levels of *NFIB*, *NFIC*, and *NFIX* RNA in U251 compared with U87 MG cells (Fig. S1*A*) (14). Similar overall levels of NFI protein are observed in U87 and U251 MG cells using a pan-specific antibody (14).

As observed previously for the *FABP7* promoter (14, 15), protein–DNA complexes are formed using both U87 and U251 nuclear extracts. U87 protein–DNA complexes migrate more slowly than those in U251, in keeping with the hyperphosphorylated state of NFIs in U87 MG cells (Fig. 2*B*) (14). A 100-fold molar excess of either cold C2 or C3 oligonucleotide competitor effectively prevented binding of proteins to the C2 probe in both U251 and U87 MG cells. Similar results were obtained with the C3 probe, except that the lower band was competed out with excess C3, but not excess C2, oligonucleotides. Excess mutated C2* oligonucleotides (mutated at two conserved G residues in the first half of the palindrome; Fig. 1*C*) competed to some extent with the radiolabeled C2 probe, resulting in a reduced signal compared with cold C2 (WT) competitor (Fig. 2*B*). Excess mutated C3* oligonucleotides (mutated at two conserved G residues in the first half of the palindrome and two C residues in the second half of the palindrome; Fig. 1*C*) failed to compete with the C3 probe (Fig. 2*B*). As expected, oligonucleotides containing a consensus NFI-binding site effectively competed with the C2 and C3 probes for protein binding, but oligonucleotides containing a consensus AP2-binding site did not compete with either probe. These data indicate that (i) an intact NFI consensus binding site is required for protein binding to C2 and C3 probes and (ii) the lower C3–protein complex (indicated by the asterisk), although specific to the C3 oligonucleotide, does not involve NFI binding.

In vitro binding of NFI to C2 and C3 oligonucleotides

To investigate whether NFI is a component of the C2 or C3 oligonucleotide–protein complexes observed in Fig. 2, we carried out supershift assays using antibodies targeting each of the four NFIs. As there are no reliable sources for some of the NFI antibodies, we generated our own anti-NFI antibodies. These NFI antibodies showed moderate (anti-NFIA, -NFIB,

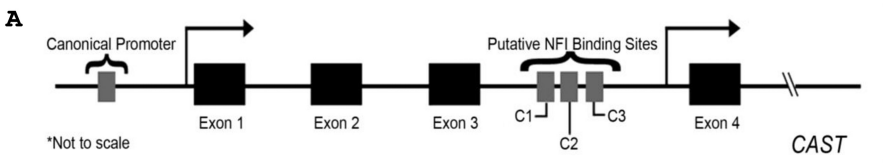

B

		NFI Consensus Binding Sequence			
		TTGGC	**(N_{3-6})**	**GCCAA**	
C1	AGGGAA	*CAT***GC**	ACGCA	**GCCCA**	GTG
	TT	**GTACG**	TGCGT	**CGGGT**	CACAAGAA
C2	GGTGC	**CTGGC**	AAGAG	**GCCAG**	GAGGA
	G	**GACCG**	TTCTC	**CGGTC**	CTCCTGCAC
C3	CCCATC	**CTGGC**	TCACTT	**GCCAG**	GAC
	AG	**GACCG**	AGTGAA	**CGGTC**	CTGGACG

C

C2*	GG	TGC	**CTaaC**	AAGAG	**GCCAG**	GAG	GA		
		G	**GAttG**	TTCTC	**CGGTC**	CTC	CTG	CAC	
C3*	CCC	ATC	**CTaaC**	TCACTT	**GaaAG**	GAC			
		AG	**GAttG**	AGTGAA	**CttTC**	CTG	GAC	G	
NFI		ATT	**TTGGC**	TTGAA	**GCCAA**	TAT	G		
		TAA	**AACCG**	AACTT	**CGGTT**	ATA	C		
AP2	GAT	CGA	ACT	GAC	CGC	CCG	CGG	CCC	GT
	CTA	GCT	TGA	CTG	GCG	GGC	GCC	GGG	CA

Figure 1. *Schematic representation* of *CAST* promoters and location of predicted NFI-binding sites. *A*, the canonical and alternative *CAST* promoters located upstream of exon 1 and exon 4, respectively. The relative position of the three putative NFI-binding sites (C1, C2, and C3; not to scale) found within intron 3 are shown. *B*, comparison of the three NFI recognition elements and NFI consensus binding site. Conserved nucleotide sequences are indicated in *boldface type*. *C*, C2* and C3* represent mutated C2 and C3 NFI-binding sites, with substitutions indicated in *lowercase type*. NFI and AP2 recognition sites are positive and negative competitors, respectively, for gel shift experiments.

and -NFIC) to high specificity (anti-NFIX) toward their intended targets (Fig. S1*B*). Importantly, this panel of NFI antibodies did not cross-react with other members of the NFI family (Fig. S1*B*). Supershifted bands were observed when anti-NFIC antibody was incubated with either the C2 or C3 probe in the presence of either U87 or U251 nuclear extracts, indicating that NFIC is present in both C2– and C3–protein complexes (Fig. 3*A*). Weak supershifted bands were also observed with the anti-NFIX antibody. Although no supershifted band was detected in the presence of anti-NFIA antibody, there was a reduction in the intensity of the protein–DNA complex, suggesting interference with the binding of NFIA to the DNA probe in the presence of anti-NFIA antibody. The addition of anti-NFIB antibody to both U251 and U87 nuclear extracts resulted in faster-migrating C2– and C3–protein complexes, suggesting that binding of NFIB to anti-NFIB antibody results in the dissociation of an NFIB co-factor. Supershift experiments with anti-AP2 antibody had no effect on the migration of either the C2–protein or C3–protein complexes. These results suggest that all four NFIs may bind to C2 and C3 oligonucleotides or interact with protein–C2 or –C3 complexes, in both U87 and U251 MG cells. To verify the binding of NFIs to C2 and C3 oligonucleotides, we transiently transfected U87 and U251 MG cells with siRNA targeting NFIC and repeated the gel shift experiments. NFIC was chosen for this analysis, as it produced the strongest supershifted band. Depletion of NFIC resulted in the loss (or reduction in signal intensity) of both the shifted and supershifted bands (Fig. S2*A*), supporting the binding of NFIC to both C2 and C3 NFI-binding sites located in *CAST* intron 3.

As not all antibodies can supershift, we transiently transfected U87 and U251 MG cells with hemagglutinin (HA)-tagged NFI expression constructs and repeated the supershift assay with an anti-HA antibody. The latter antibody has previously been shown to supershift HA-tagged NFI proteins in gel shift assays (14). Western blot analysis of nuclear extracts prepared from cells transfected with each of the four HA-tagged NFI constructs revealed successful expression of HA-tagged NFIs (Fig. 3*B*). The presence of supershifted bands in extracts prepared from all four NFI transfectants indicates that C2 and C3 oligonucleotides are recognized by all four members of the NFI family in both U87 or U251 MG cells, at least when NFIs

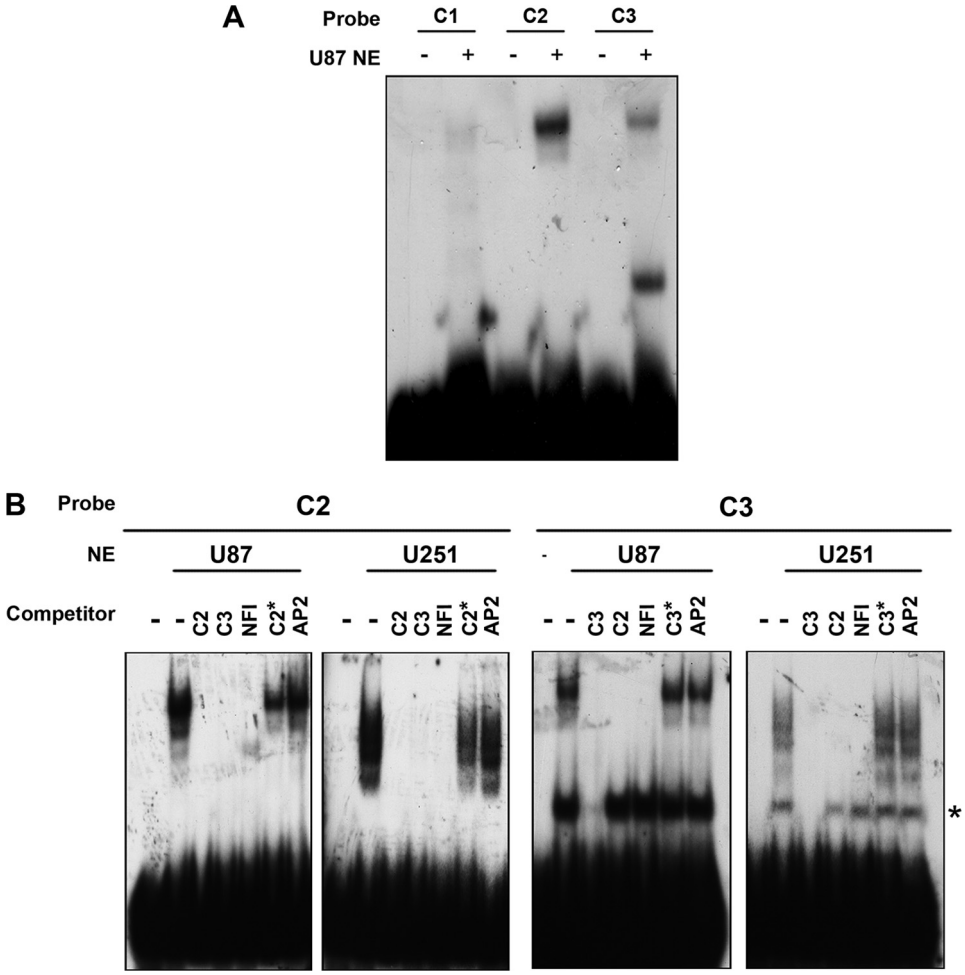

Figure 2. Gel shifts showing binding of proteins in MG cells to *CAST* NFI recognition sites. *A*, gel shift assay using ^{32}P-labeled C1, C2, and C3 double-stranded oligonucleotides with (+) or without (−) nuclear extracts (1 μg) prepared from U87 MG cells. Samples were electrophoresed in a 6% polyacrylamide gel in 0.5× TBE buffer to separate free DNA probes and DNA–protein complexes. *B*, gel shift assays using nuclear extracts from U87 or U251 MG cells (1 μg/lane) and ^{32}P-labeled C2 and C3 oligonucleotides. When indicated, 100× unlabeled WT (C2, C3, NFI, and AP2) or mutated (C2* and C3*) competitors were added to the reaction. Samples were electrophoresed in a 6% polyacrylamide gel in 0.5× TBE buffer to separate free DNA probes and DNA–protein complexes. Gels are representative of three independent experiments.

are ectopically expressed (Fig. 3*C*). The migration patterns of the shifted complexes were similar in both U87 and U251 MG cells, suggesting that exogenous NFIs are not subjected to the same phosphorylation/dephosphorylation process as endogenous NFIs.

Binding of NFI to CAST in intact chromatin

To explore the binding of NFI to *CAST* intron 3 in the context of native chromatin, we performed ChIP analysis using two NFI- hyperphosphorylated (U87 and T98) and two NFI-hypophosphorylated (M049 and U251) MG cell lines (15). Cells were cross-linked with formaldehyde to capture DNA–protein interactions. NFI-bound DNA was then immunoprecipitated with an anti-NFI antibody (obtained from Dr. Naoko Tanese, New York University Medical Center) that preferentially recognizes NFIC but also binds to the other NFIs (14). The rationale for using this antibody is that NFIC appears to be a major component of both the protein–C2 and protein–C3 complexes based on supershift (Fig. 3*C*) and NFIC-knockdown experiments (Fig. S2*A*). Rabbit IgG served as the negative control for these ChIP experiments. ChIP DNA was purified and PCR-amplified with primers flanking C2 or C3 NFI recognition sites (Table 1). DNA bands were detected in all four cell lines using primers flanking C3; however, PCR products were only detected in T98 and U87 using primers flanking C2 (Fig. 4*A*). The absence of DNA bands in the IgG control lanes combined with the absence of DNA bands using *GAPDH* primers in the NFI lanes, supports specific interaction between the anti-NFI antibody and the C2 and C3 NFI-binding sites.

For quantitative analysis of ChIP products, we performed quantitative PCR (qPCR) on chromatin immunoprecipitated DNA using primers flanking C2 and C3 recognition sites (Table 1). Primers to the *GAPDH* promoter served as the negative control. In agreement with our qualitative analysis, binding to C3 oligonucleotides was observed in all four cell lines, whereas binding to C2 was only observed in T98 and U87 MG cell lines (Fig. S2*B*). As both C2 and C3 reside in intron 3, our results suggest that NFI occupies an alternative promoter upstream of *CAST* exon 4, with NFI binding C3 regardless of its phosphorylation status. In contrast, C2 is only bound by hyperphosphorylated NFI based on both qualitative and quantitative ChIP data.

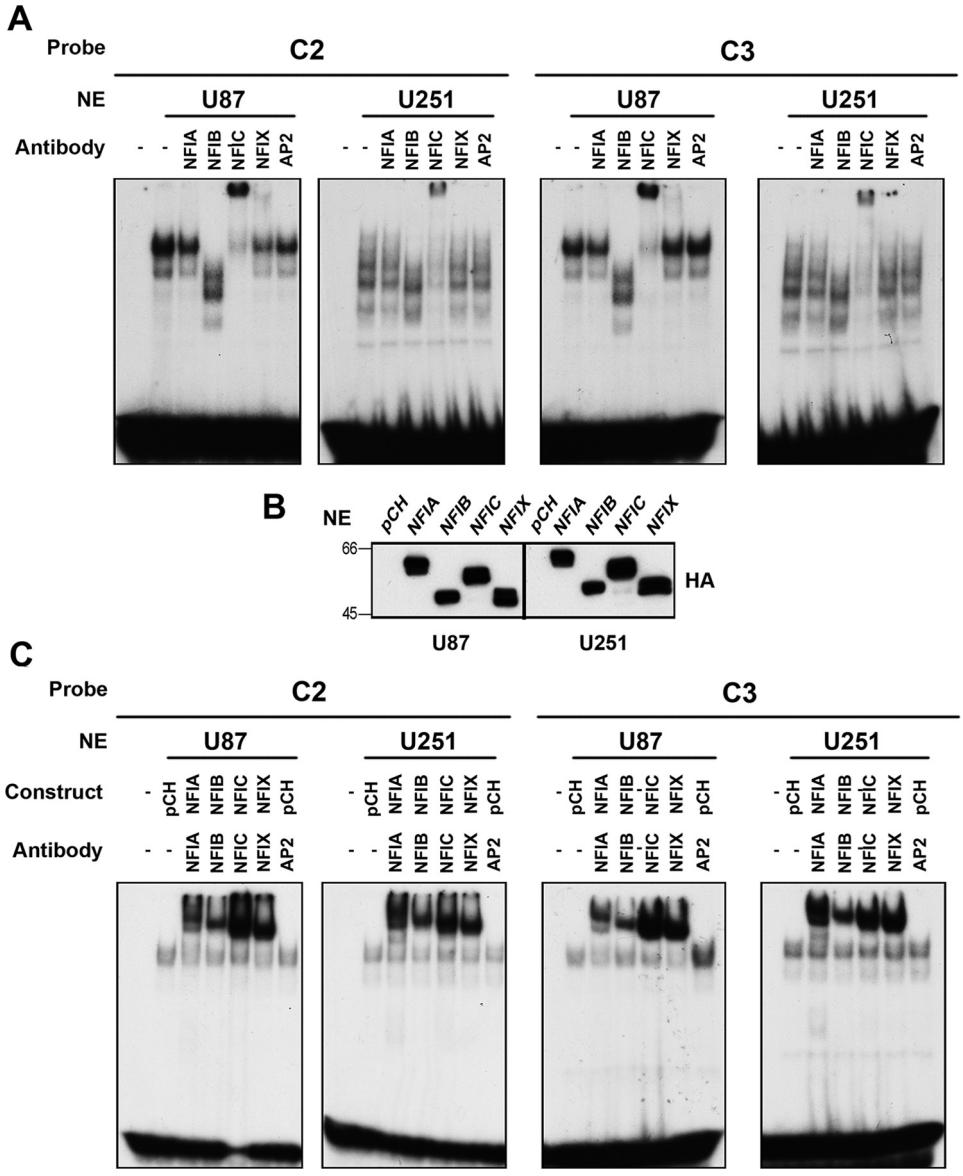

Figure 3. Binding of NFIs to the two *CAST* NFI-binding sites in intron 3. *A*, supershift assays were carried out with 4 μg of nuclear extracts prepared from U87 or U251 MG cells and ^{32}P-labeled C2 and C3 oligonucleotides. NFIA, NFIB, NFIC, or NFIX antibodies were added to the reactions as indicated. Anti-AP2 antibody served as a nonspecific control. Samples were electrophoresed in a 6% polyacrylamide gel in 0.5× TBE buffer to separate free DNA probes and DNA–protein complexes. Gels are representative of three independent experiments. *B*, Western blot analysis of U87 and U251 MG cells transiently transfected with HA-tagged NFI expression constructs. Empty vector (pCH) served as negative control. Nuclear extracts were prepared using the NE-PER nuclear and cytoplasmic extraction kit (Thermo Fisher Scientific). Proteins were transferred to nitrocellulose membranes and immunoblotted with anti-HA antibody. *C*, nuclear extracts were prepared from U87 or U251 cells transfected with the indicated HA-tagged NFI expression constructs. Four μg of nuclear extracts were incubated with ^{32}P-labeled C2 and C3 oligonucleotides, and anti-HA antibody was included where indicated. Anti-AP2 antibody served as a negative control. Samples were electrophoresed in a 6% polyacrylamide gel in 0.5× TBE buffer to separate free DNA probes and DNA–protein complexes. Gels are representative of two independent experiments.

Binding of RNA polymerase II to CAST canonical promoter and intron 3 region in intact chromatin

To assess the transcriptional states of the *CAST* canonical (CP) and putative alternative (ALT) promoters in U87 (NFI-hyperphosphorylated) *versus* U251 (NFI-hypophosphorylated) MG cells, we performed ChIP analysis with an antibody to RNA polymerase II (Pol II) that specifically recognizes a phosphorylated Ser-5 residue in its C-terminal domain repeats (YSPTSPS). This phosphorylated form of RNA Pol II occupies the proximal promoter regions of transcriptionally active genes (37). We used mouse IgG as a control for antibody specificity. We also included two additional controls: a region of the active *GAPDH* proximal promoter that contains the TATA box bound by RNA Pol II (positive control) and an upstream region of the *GAPDH* promoter that is not bound by RNA Pol II (negative control).

In U87 MG cells, RNA Pol II showed significantly increased occupancy at the canonical *CAST* promoter compared with the alternative *CAST* promoter in intron 3. In U251 MG cells, RNA Pol II occupied both the canonical (primers flanking a proximal TATA box upstream of exon 1) and alternative (primers flanking a proximal TATA box upstream of exon 4) *CAST* promoters (Fig. 4*B*; primers listed in Table 1). These results indicate that the alternative *CAST*

Table 1
Primer sequences

Assay	Target	Sense primer	Antisense primer
RT-(q)PCR	*NFIA*	CTCCACAAAGCGCCTCAAG	CATCAGGGCAGACAAGTTGG
	NFIB	GAAGTCCAAGCCACAATGATC	GATGCAGAGCTGAACAATGG
	NFIC	GATGCAGAGCTGAACAATGG	CATCTCTGTCTTCTTCACCG
	NFIX	GTTCAAACCAGCAAGGAGATG	CGTCATCAACAGGGCTCTC
	ACTB	CTGGCACCACACCTTCTAC	CATACTCCTGCTTGCTGATC
qPCR	*CAST* exon 1--exon 2	ACAACTGCAAGCTAGATCTG	CTTTCTTTTCTCCTGGTTTGG
	CAST exon 4--exon 5	GTGTCAGCTTCCTCTGGTG	CTGTTTTTTTGTGTTTTTTCTTGTT
	CAST exon 16--exon 18	AGTGTGGTGAGGATGATGAAA	TTTTCAGTTGGCTTAGATGGTT
	GAPDH	GAGATCCCTCCAAAATCAA	CACACCCATGACGAACAT
ChIP	*CAST* C2	TGTGCCAAGTTCCGAGCCAA	TAGAAGCAGGGGCAGAGGAA
	CAST C3	TGTAGTGGCGCAATGGATGA	CTGGGCAATGTAGTGAGACC
	CAST canonical promoter	GTTCTCCTCCCCATAAAAGTT	AGGAAGCGGATCACAAAAACA
	CAST alternative promoter	ATTCATTATGTGCCAGGGAGT	AAATCTAGTAGGAGGTGGTGT
	GAPDH positive control	TACTAGCGGTTTTACGGGCG	TCGAACAGGAGGAGCAGAGAGCGA
	GAPDH negative control	GAACCAGCACCGATCACC	CCAGCCCAAGGTCTTGAG
RLM RACE	Outer RNA adapter	GCTGATGGCGATGAATGAACACTG	
	Inner RNA adapter	CGCGGATCCGAACACTGCGTTTGCTGGCTTTGATG	
	CAST exon 4		TACTGGAAGACTTGCTGGTTGC
	CAST exon 8		ACTTCCTGTATCTGATGCCTGC
	CAST exon 14		CTTCTCCACCTTTCTTTTCT

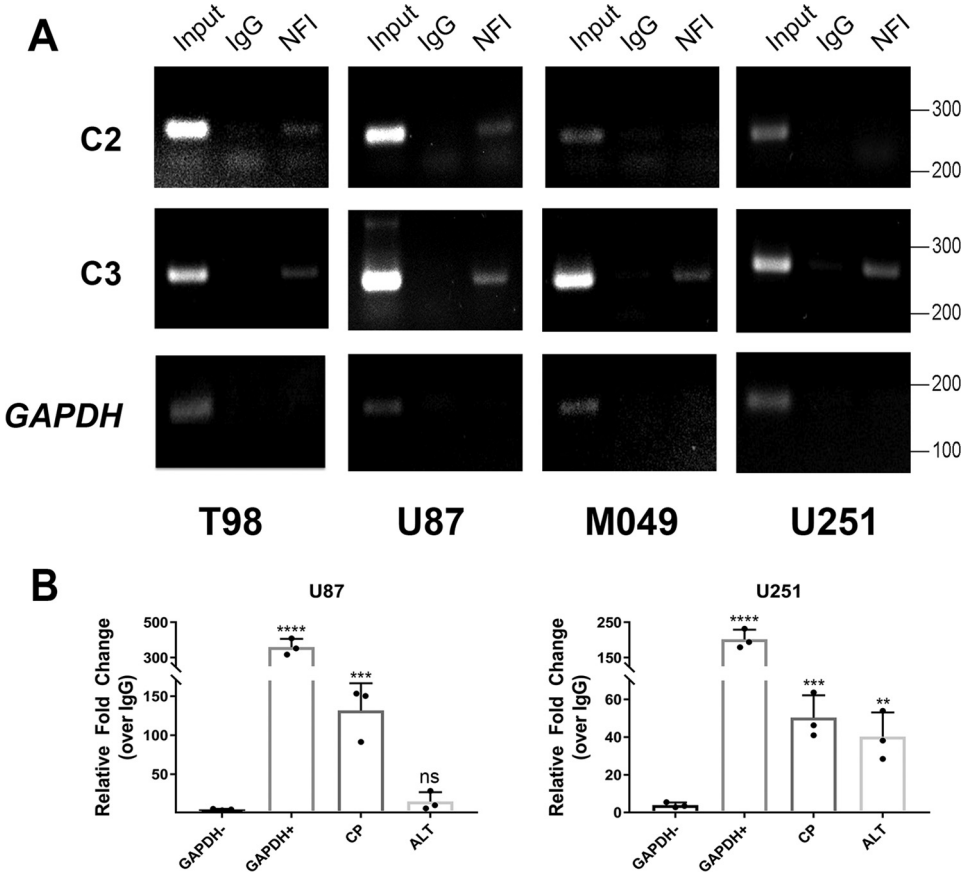

Figure 4. Binding of NFIs to the two *CAST* NFI-binding sites in intron 3. ChIP analyses were performed with 2 μg of a pan-specific anti-NFI (from Dr. Naoko Tanese) antibody (*A*) or an anti-RNA polymerase II antibody (*B*) using some or all of the following cell lines: NFI-hyperphosphorylated T98 and U87 and NFI-hypophosphorylated M049 and U251 MG cell lines. *A*, primers targeting C2 and C3 were used for PCR amplification of *CAST* NFI-binding sites (Table 1). Primers to a nonrelevant region of *GAPDH* promoter served as a negative control. Input consists of genomic DNA obtained after sonication but before immunoprecipitation. The band in input DNA is of the expected size and serves as a positive control. *B*, specific primers were used to qPCR-amplify either the *CAST* CP or ALT promoter region, each of which contains a TATA box (Table 1). Primers to an upstream region of the *GAPDH* proximal promoter served as a negative control (Table 1). Primers to the *GAPDH* proximal promoter region containing the TATA box served as a positive control (Table 1). Scatter plots in *B* were generated by normalizing signals obtained with NFI or RNA Pol II antibodies against those generated by IgG. Each ChIP experiment was carried out three times. qPCR data are presented as mean ± S.D. (*error bars*). **, $p < 0.01$; ***, $p < 0.001$; ****, $p < 0.0001$; ns, not significant.

promoter located in intron 3 is active primarily in NFI-hypophosphorylated U251 MG cells. Thus, our combined ChIP data suggest that engagement of hypophosphorylated NFI at C3 activates *CAST* intron 3 alternative promoter, whereas occupation of C2 and C3 by hyperphosphorylated NFI inactivates *CAST* intron 3 alternative promoter.

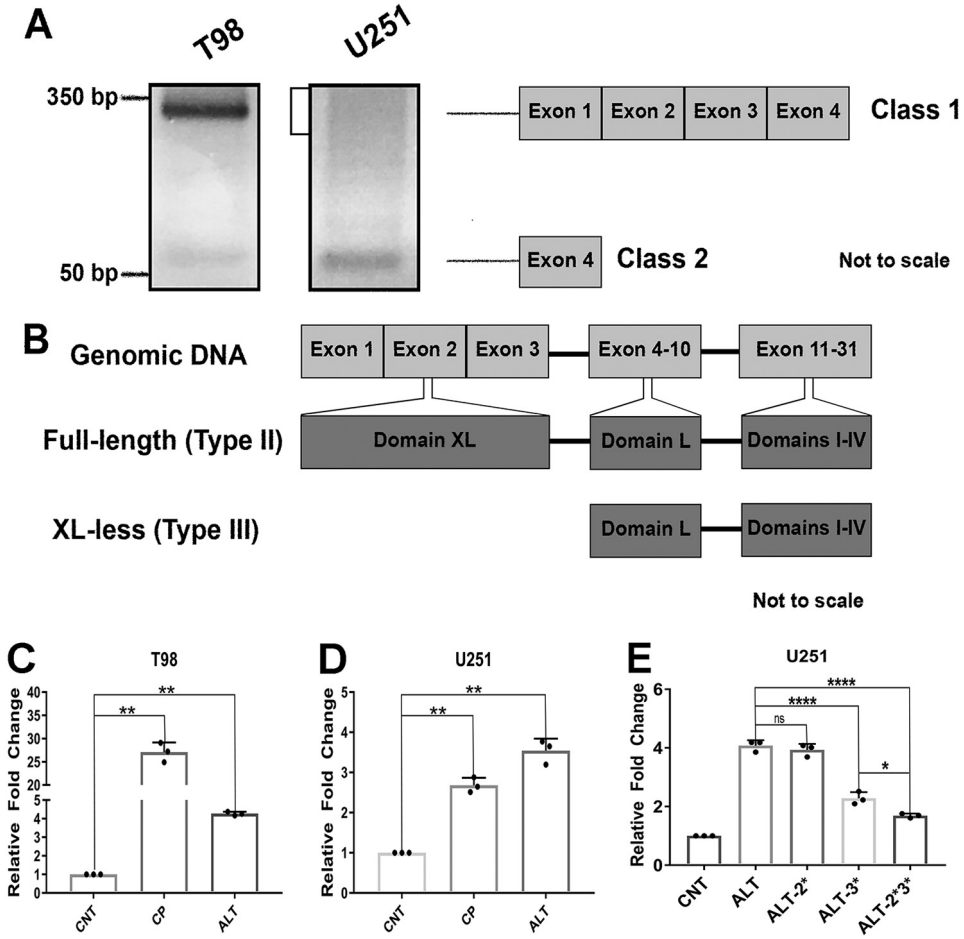

Figure 5. CAST promoter activity and calpastatin isoform expression in MG cells. *A*, RLM RACE was carried out using 5 μg of total RNA isolated from NFI-hyperphosphorylated (T98) or NFI-hypophosphorylated (U251) MG cells. Antisense primer targeting exon 14 of the *CAST* gene was used for reverse transcription. Nested PCR amplification was carried out with 5′-ligated outer and inner primers and antisense primers targeting exons 8 and 4 of the *CAST* gene, respectively. PCR products were electrophoresed in 3% Metaphor (FMC Bioproducts) agarose gel, visualized with ethidium bromide, excised, purified, and sequenced using the BigDye Terminator version 3.1 cycle sequencing kit (Thermo Fisher Scientific). Exon composition of the isolated DNA products based on sequence analysis is indicated on the *right*. *B*, domain composition of XL-containing (full-length/type II) and XL-less (type III) calpastatin isoforms. T98 (*C*) and U251 (*D*) MG cells were transiently transfected with luciferase reporter constructs containing the CP (~2000 bp upstream of *CAST* exon 1), ALT (in intron 3 containing the NFI-binding sites; ~4000 bp upstream of *CAST* exon 4), or empty vector (CNT). Luciferase activity was measured using the Luciferase Assay System (Promega) and the FLUOstar microplate reader (BMG LABTECH). Relative -fold change was calculated relative to the empty vector control. Scatter plots show data from three independent experiments. *E*, U251 MG cells were transiently transfected with luciferase reporter constructs containing the WT ALT or constructs containing mutation at C2 (ALT-C2*), C3 (ALt-C3*), or both C2 and C3 (ALT-C2*C3*) NFI-binding sites. Luciferase activity was measured 48 h post-transfection as described above. *p* values were obtained from one-way analysis of variance statistical analysis of three independent experiments. *, $p < 0.05$; **, $p < 0.01$; ****, $p < 0.0001$; ns, not significant.

CAST variant expression in MG cells

Our combined gel shift and ChIP data indicate that C2 and C3 are *bona fide* NFI-binding sites. To address the possibility of an alternative *CAST* transcription start site downstream of these binding sites, we carried out 5′-RNA ligase-mediated rapid amplification of cDNA ends (5′-RLM RACE) using total RNA prepared from T98 (hyperphosphorylated NFI) and U251 (hypophosphorylated NFI) MG cells. cDNAs underwent two rounds of PCR amplification using nested primer pairs designed to amplify transcripts initiating at exon 1 (class 1 variants) or exon 4 (class 2 variants) (Table 1). Two main bands were identified in T98, a strong band at ~340 bp and a weak band at ~60 bp (Fig. 5*A*). The only clear band detected in U251 cells was ~60 bp. Based on DNA sequencing analysis, the 340-bp DNA fragment contains exons 1–4 sequences, whereas the 60-bp band only has exon 4 sequences (Fig. 5*A*). These results are consistent with the presence of two *CAST* promoters in MG cells, with the canonical promoter upstream of exon 1 directing the expression of the longer form of *CAST* found (class 1 variant), and the NFI-bound alternative promoter upstream of exon 4 directing the expression of the shorter form of *CAST* (class 2 variant) (Fig. 5*B*). As ChIP data demonstrate RNA Pol II occupancy at both the canonical and alternative *CAST* promoters in U251 MG cells, the smear observed at ~350 bp (see *square bracket* in Fig. 5*A*) may represent transcription start site stuttering in NFI-hypophosphorylated U251 cells.

CAST promoter activity in MG cells

To further examine the utilization of the two promoters controlling the expression of class 1 and class 2 *CAST* variants, we transfected T98 and U251 MG cells with pGL3 luciferase reporter gene constructs driven by either the CP (−1990 to +50 with +1 indicating the start of exon 1) or ALT promoter

(−4026 to +20 with +1 indicating the start of exon 4). The empty (promoterless) pGL3 vector served as the negative control. We then assessed the activity of *CAST* canonical and alternative promoters by measuring luciferase activity. In T98 MG cells (hyperphosphorylated NFI), the canonical promoter generated a 27-fold increase in luciferase activity compared with empty vector (Fig. 5*C*). In comparison, luciferase activity driven by the NFI-bound alternative promoter was increased 4.3-fold relative to control levels. In contrast, luciferase activity was increased by 2.7- and 3.5-fold when U251 (hypophosphorylated NFI) MG cells were transfected with vector containing the *CAST* canonical promoter and alternative promoter, respectively (Fig. 5*D*). These results are generally consistent with our RLM RACE and ChIP data in that they demonstrate (i) strong bias toward utilization of the *CAST* canonical promoter in NFI-hyperphosphorylated T98 cells and (ii) similar utilization of both canonical and alternative promoters in NFI-hypophosphorylated U251 MG cells.

Next, we tested the effect of mutating the C2 and C3 NFI-binding sites on luciferase activity. For these experiments, we generated luciferase reporter constructs with NFI-binding site mutations at C2 (ALT-C2*), C3 (ALT-C3*), or both C2 and C3 (ALT-C2*C3*). In U251 MG cells, luciferase activity driven by the ALT-C2* promoter was not statistically significantly different from that of WT alternative promoter, in agreement with our ChIP results indicating that C2 is not bound by NFI in these cells (Fig. 5*E*). Mutation of C3 resulted in lower luciferase activity (0.56-fold) compared with WT alternative promoter ($p < 0.0001$), suggesting that C3 is required for NFI-mediated positive regulation of *CAST* alternative promoter activity. Mutating both the C2 and C3 sites resulted in a slight decrease ($p < 0.05$) in luciferase activity compared with mutating C3 alone. These results are in agreement with C3 being the main effector of *CAST* alternative promoter activity in NFI-hypophosphorylated U251 MG cells, in keeping with our ChIP data (Fig. 4).

Expression of calpastatin isoforms in MG cells

To understand how the regulation of *CAST* by NFI affects calpastatin protein, we examined expression of different calpastatin isoforms in NFI-hyperphosphorylated (U87) and NFI-hypophosphorylated (U251) MG cells using a pan-specific anti-calpastatin antibody. U87 MG cells primarily expressed the full-length calpastatin (indicated by an *asterisk* in Fig. 6*A*), which has been shown to migrate as a ~145 kDa band in SDS-PAGE (32). The full-length calpastatin is a translational product of class 1 *CAST* variants, which in turn is directed by the canonical promoter. In contrast, U251 MG cells expressed both the full-length and XL-less isoform (indicated by the *arrow* in Fig. 6*A*), which has been shown to migrate as a ~135 kDa band (32). The absence of the latter in U87 MG cells suggests that the ~135 kDa band is a translational product of class 2 *CAST* variants, which is directed by the alternative promoter. The ratio of the 145 kDa to 135 kDa bands is ~1:1 (Fig. 6*A*). In agreement with our previous observations, these results support (i) preferential utilization of the *CAST* canonical promoter in NFI-hyperphosphorylated MG cells and (ii) utilization of both the *CAST* alternative and canonical promoters in MG cells with hypophosphorylated NFI. To test the specificity of the calpastatin antibody, we transfected U251 MG cells with siRNAs targeting different regions of *CAST* RNA (exon 4 or exon 16). Western blot analysis shows one strong band at ~140 kDa, along with several weaker bands, all of which disappear upon *CAST* siRNA transfection (Fig. 6*B*).

Regulation of CAST by NFI

We also examined how NFI regulates endogenous *CAST* mRNA levels by depleting U251 and U87 MG cells of specific NFIs using siRNAs to each of the four NFIs (Fig. 6*C*). Endogenous *CAST* variant analysis was carried out using primers that span *CAST* exons 1 and 2 (E1-E2) to measure class 1 *CAST* variants, primers that target exons 4 and 5 (E4-E5) to measure levels of combined class 1 and 2 *CAST* variants, and primers that target exons 16 and 18 (E16-E18) to measure levels of all calpastatin variants as this region encodes domain II (second inhibitory domain) of calpastatin, which is commonly found in brain calpastatin isoforms (see Table 1 for primer sequences).

There was no significant difference in levels of class 1 *CAST* transcripts upon knockdown of any of the NFIs in U87 MG cells (Fig. 6*D*). Knockdown of either NFIB or NFIC in U87 MG cells significantly reduced the levels of combined class 1 and 2 *CAST* transcripts to 0.55-fold ($p < 0.0001$) or 0.73-fold ($p < 0.001$) of control levels, respectively (Fig. 6*E*). Depletion of NFIB, but not NFIA, NFIC, or NFIX, reduced total *CAST* RNA levels in U87 MG cells to 0.61-fold ($p < 0.0001$) of control levels (Fig. 6*F*). These data indicate that NFIB may act as a positive regulator of class 2 *CAST* transcript levels in NFI-hyperphosphorylated U87 MG cells. However, the interpretation of these data is confounded by the following factors: (i) the complex expression profile of *CAST* RNAs, (ii) cross-talk between the different NFIs (*e.g.* knockdown of NFIB decreases *NFIC* levels) (Fig. 6*C*), and (iii) the low levels of NFIB in U87 MG cells based on Northern blot analysis (14) and RT-qPCR (Fig. S1*A*).

Depletion of either NFIC or NFIX in NFI-hypophosphorylated U251 MG cells had no significant effect on levels of class 1 *CAST* transcripts (Fig. 6*G*). However, NFIA- and NFIB-depleted cells showed a small increase in class 1 transcripts, by 1.48 ($p < 0.05$) and 1.22-fold ($p < 0.05$), respectively. Depletion of NFIA, but not NFIB, NFIC, and NFIX, in U251 MG cells significantly reduced levels of combined class 1 and 2 *CAST* transcripts (0.47-fold decrease compared with control; $p < 0.01$) (Fig. 6*H*). Knocking down either NFIC or NFIX was accompanied by increased levels of total (E16-E18–containing) *CAST* transcripts, by 1.34-fold ($p < 0.05$) and 1.99-fold ($p < 0.05$), respectively (Fig. 6*I*). Overall, our data in U251 MG cells are consistent with all four NFIs playing some role in regulating the complement of *CAST* variants expressed in NFI-hypophosphorylated MG cells. NFIA in particular appears to act as a weak negative regulator of class 1 *CAST* transcripts and a strong positive regulator of class 2 *CAST* transcripts.

Changes in calpastatin subcellular localization upon NFI depletion

One of the best-characterized roles of calpastatin is inhibition of calpain protease activity. In turn, the subcellular location of calpain determines its physiological functions, with calpain

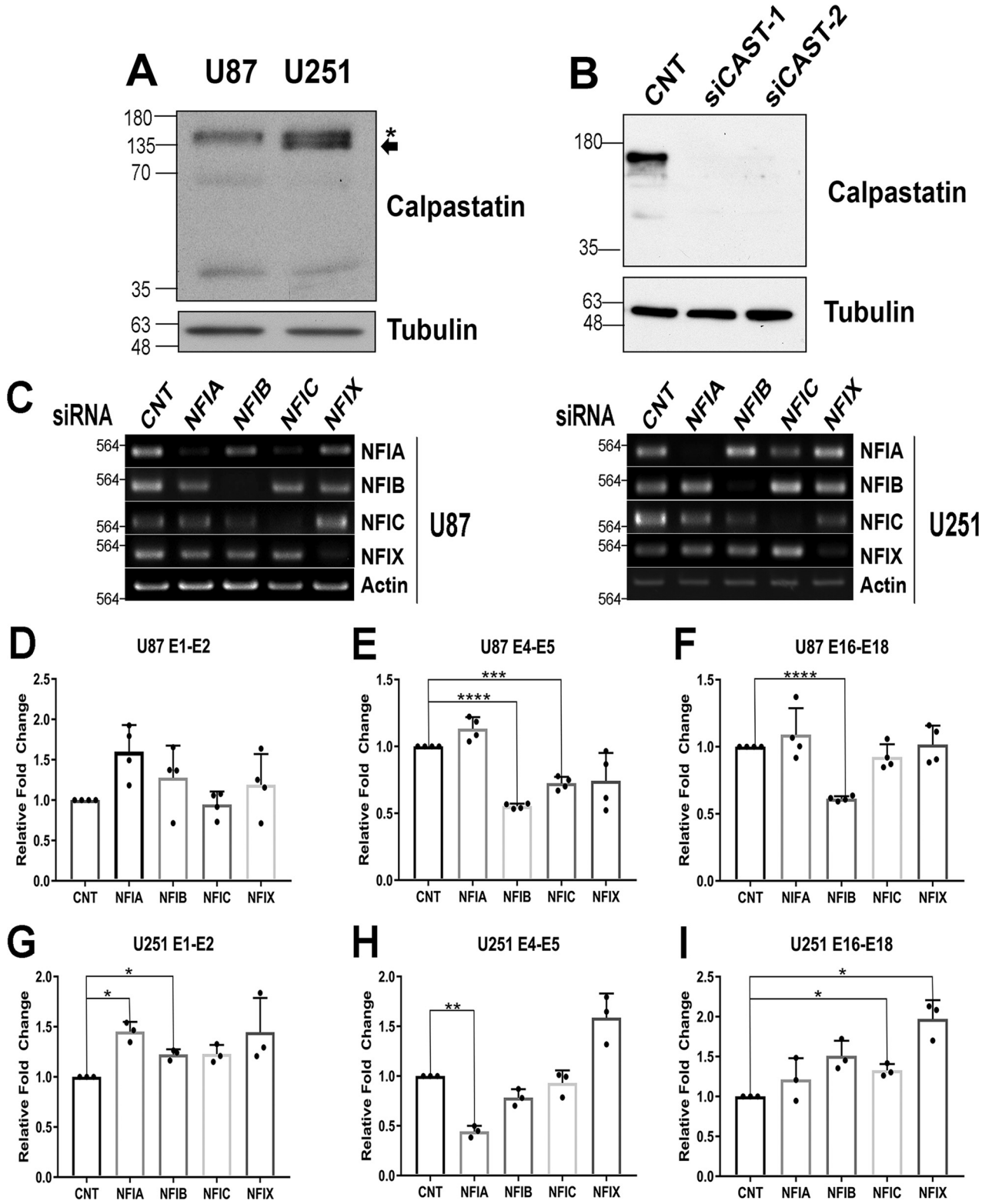

Figure 6. CAST variants and calpastatin isoform expression in MG cells. Whole-cell extracts from nontransfected U87 and U251 cells (*A*) or U251 MG cells transiently transfected with scrambled (control; *CNT*) or siRNAs targeting *CAST* exon 4 (si-CAST-1) and exon 16 (siCAST-2) (*B*) were electrophoresed in a 15% SDS-polyacrylamide gel at 180 V for 75 min and then transferred to a nitrocellulose membrane. Blots were immunostained with rabbit polyclonal anti-calpastatin antibody (1:10,000; Santa Cruz Biotechnology) or mouse anti-α-tubulin antibody (1:100,000; Hybridoma Bank) followed by horseradish peroxidase–conjugated secondary antibody (1:50,000). The signal was detected using the Immobilon Western detection reagent. *C*, RT-PCR showing the knockdown efficiencies of siRNAs targeting specific NFIs in U87 and U251 MG cells. *D–I*, quantitative PCR analysis using cDNAs prepared from U87 (*D–F*) or U251 (*G–I*) MG cells transiently transfected with siRNAs targeting specific NFIs as indicated. cDNAs were amplified with primers targeting exons 1 and 2 (*D* and *G*), exons 4 and 5 (*E* and *H*), or exons 16 and 18 (*F* and *I*) of the *CAST* gene. *GAPDH* was used as a control for variation in cDNA concentration. Scatter plots show -fold changes relative to scrambled siRNA control (set at 1) in three independent experiments. *Bars*, mean ± S.D. (*error bars*) for three independent experiments. *, $p < 0.05$; **, $p < 0.01$; ***, $p < 0.001$; ****, $p < 0.0001$.

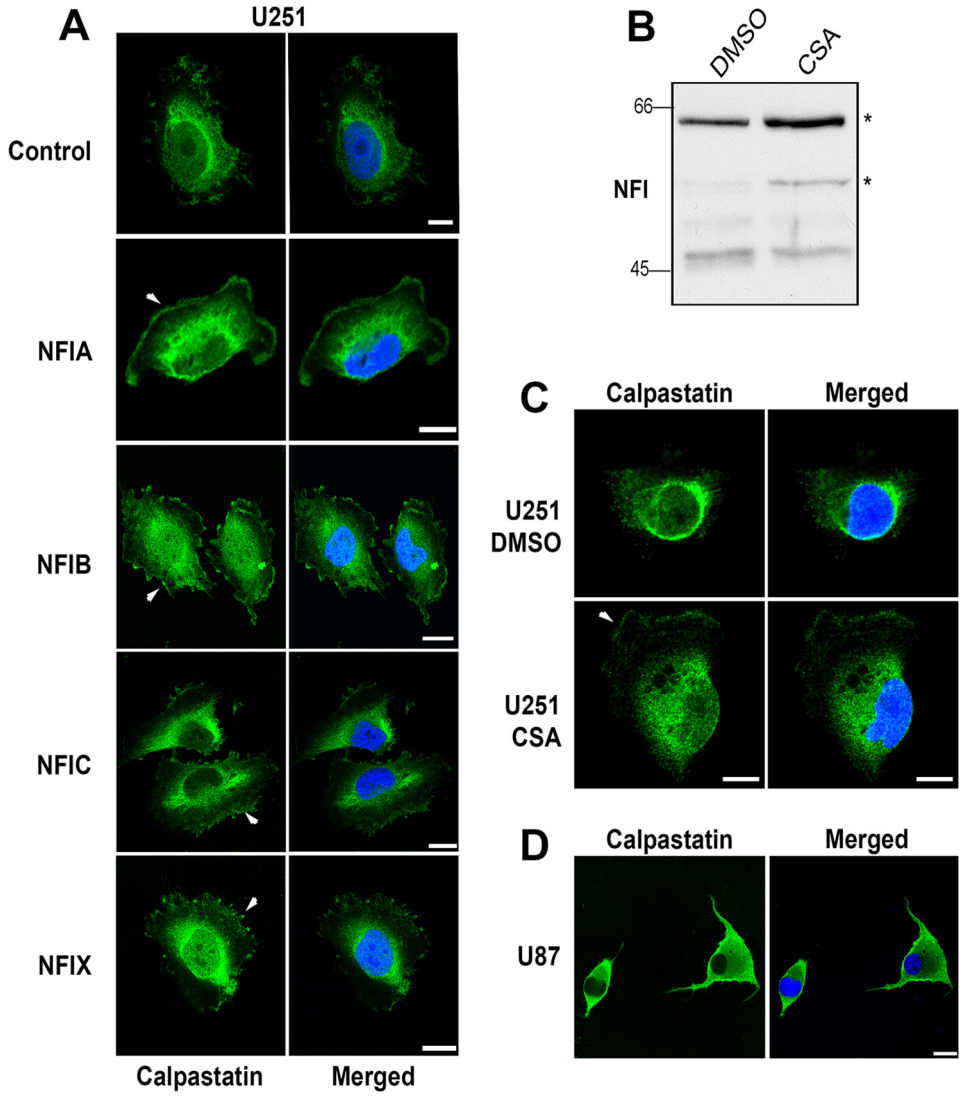

Figure 7. Changes in calpastatin subcellular localization upon NFI knockdown or modification of NFI phosphorylation. *A*, U251 MG cells were transiently transfected with siRNAs targeting the indicated NFIs and then plated on coverslips. After 48 h, cells were fixed with 4% paraformaldehyde and immunostained with a polyclonal anti-calpastatin antibody (1:100; Santa Cruz Biotechnology) followed by Alexa 488–conjugated secondary antibody (*green signal*). Nuclei were stained with 4′,6-diamidino-2-phenylindole (*blue*), and images were acquired by confocal microscopy using a 40×/1.3 numerical aperture oil immersion lens. *Bars*, 10 μm. All images are representative of the majority of cells observed under each condition. The *arrowheads* point to the calpastatin signal at the plasma membrane. *B*, U251 MG cells were treated with 1 μM CSA for 1 h at 37 °C. Nuclear extracts were electrophoresed in SDS-polyacrylamide gels and electroblotted onto nitrocellulose membranes. Blots were immunostained with a mouse pan-specific anti-NFI antibody (1:1000; Santa Cruz Biotechnology), followed by horseradish peroxidase–conjugated secondary antibody (1:50,000). The signal was detected using the Immobilon Western detection reagent. The *asterisks* indicate hyperphosphorylated forms of NFI. CSA-treated U251 MG cells (*C*) or U87 MG cells transfected with scrambled (control) siRNAs (*D*) were fixed, immunostained, and visualized as described in *A*. *Bars*, 20 μm (*C*) or 10 μm (*D*). All images are representative of three independent experiments.

frequently found at the plasma membrane, where it cleaves downstream targets, many of which are migration-related effectors (38, 39). Because direct binding of calpastatin to calpain is required to inhibit calpain's protease activity (24), we examined the effect of NFI depletion on calpastatin subcellular localization in NFI-hypophosphorylated U251 MG cells, which express both full-length and XL-less calpastatin.

In U251 MG cells, calpastatin was primarily present in the nucleus and cytoplasm, with increased immunostaining in the perinuclear region (Fig. 7*A*) (Fig. S3). NFIA and NFIC knockdown resulted in increased accumulation of calpastatin at the plasma membrane. NFIB- and NFIX-depleted U251 cells showed increased calpastatin immunostaining at the plasma membrane in structures resembling lamellipodia as well as higher levels of nuclear calpastatin.

To examine the importance of NFI phosphorylation state for calpastatin subcellular localization, we treated U251 MG cells with 1 μM cyclosporin A (CSA), an inhibitor of calcineurin that promotes NFI hyperphosphorylation (21). CSA-treated U251 MG cells showed increased levels of hyperphosphorylated NFI (indicated by the *asterisks*) (Fig. 7*B*). Immunostaining analysis revealed a perinuclear localization for calpastatin in U251 MG cells treated with DMSO vehicle. CSA-treated cells showed a more diffuse calpastatin immunostaining pattern in the cytoplasm with accumulation at the plasma membrane (Fig. 7*C* and Fig. S4*A*). For comparison, we immunostained U87 MG cells with anti-calpastatin antibody. Calpastatin was found throughout the cytoplasm and at the plasma membrane (Fig. 7*D* and Fig. S4*B*). Thus, the subcellular distribution of calpastatin in U251 MG cells with induced NFI hyperphosphorylation shows

some similarity with that of NFI-hyperphosphorylated U87 MG cells.

When combined with our NFI promoter analyses, these immunostaining data support a regulatory link between NFI hypophosphorylation and (i) utilization of the *CAST* alternative promoter, (ii) transcription of class 2 *CAST* variants, (iii) expression of XL-less calpastatin, (iv) loss of calpastatin at the plasma membrane, and (v) perinuclear localization of calpastatin.

Discussion

Many studies have demonstrated the importance of NFIs in the development of the central nervous system, including the regulation of neural cell differentiation and gliogenesis (40, 41). In particular, NFIA and NFIB are required for the initiation of gliogenesis and later promote the differentiation of astrocytes (42, 43). In MG, NFI regulates *FABP7*, the expression of which coincides with increased tumor cell migration, tumor infiltration, and worse clinical prognosis (10, 12, 13, 44). In the context of MG cells, NFI transcriptional activity is regulated by its phosphorylation state (45), with dephosphorylation of NFI mediated by the calcineurin phosphatase, a well-known target of calpain (21, 46, 47).

We show here that NFI regulates transcription of the *CAST* gene, which encodes calpastatin, a highly specific inhibitor of calpain (24). Similar to NFI, the calpains also play a role in brain development, with μ-calpain (calpain 1) suppressing neural differentiation and m-calpain (calpain 2) inducing glial differentiation (48). Furthermore, limited proteolysis of calpain targets is required for many aspects of tumor cell migration, including focal adhesion turnover (49), cytoskeleton remodeling (50), invadopodia formation (51), and lamellipodia stabilization at the migration edge (52). Notably, m-calpain is essential for MG infiltration of the brain in zebrafish (53). The convergence of NFI and calpastatin/calpain in normal brain development and regulation of cell migration suggests possible cross-talk between these two pathways, with NFI regulating expression of specific *CAST* variants and calcineurin regulating NFI activity.

Overexpression of calpastatin protects cells from both calpain-mediated oxidative and proteolytic stress (54, 55), whereas depletion of calpastatin is associated with human neurodegenerative disorders, including Alzheimer's disease (56). Whereas these reports highlight the importance of calpastatin, little is known about the regulation of calpastatin itself in the cell. Our combined data, including gel shift assays, supershift assays, ChIP analysis, reporter gene assays, and analysis of *CAST* mRNA variants and calpastatin isoform expression, reveal a complex NFI-mediated mechanism for regulation of *CAST* in human MG cells. In particular, we identified two NFI-binding sites located in human *CAST* intron 3, ~4 kb upstream of exon 4, that drive expression of a *CAST* transcript variant that excludes the XL domain of calpastatin.

Bovine and murine *CAST* genes have five exons ($1x_a$, $1x_b$, 1y, 1z, and 1u) located upstream of exon 2, with the latter showing homology with human exon 4 (NCBI numbers NG_029490, NC_000079, AC_000164). Human exons 1, 2, and 3 share sequence homology with exons $1x_b$, 1y, and 1z, respectively. A functional promoter has been identified upstream of exons $1x_b$ in both bovine and murine species (25, 30). The location of NFI-binding sites upstream of human *CAST* exon 4 suggests that this intronic region may also contain an NFI-bound alternative promoter. We present evidence that the two NFI-binding sites (C2 and C3) located upstream of exon 4 are differentially occupied by NFIs in different MG cell lines. NFI binding to C2 is confined to MG cell lines with hyperphosphorylated NFI, whereas NFI binding to C3 is observed in both NFI hyper- and hypophosphorylated cell lines. The core binding palindromic sequence is identical in both C2 and C3; however, the two sites differ in the spacing between the two halves of the palindrome: 5 bp for C2 and 6 bp for C3. The length of the spacer region has been shown to influence the binding affinity of NFI to its target genes (57) and may explain differential NFI binding to C2 and C3 binding sites.

Data from RNA Pol II ChIP, luciferase reporter gene, and Western blotting analyses indicate that differential utilization of NFI-binding sites in *CAST* intron 3 results in a significantly higher ratio of XL-less calpastatin (a translational product of class 2 variants directed by the alternative promoter) *versus* full-length calpastatin (a translational product of class 1 variants directed by the canonical promoter) in migratory NFI-hypophosphorylated (U251) MG cells compared with nonmigratory NFI-hyperphosphorylated (T98 and U87) MG cells. The subcellular localization of calpastatin isoforms encoded by these variants may help explain what drives increased cell migration in MG cells. It has already been shown that calpain and calpastatin co-localize in the cytoplasm (35). When cells are treated with a Ca^{2+} ionophore, calpain relocates to the plasma membrane, where it regulates many migratory processes; however, calpastatin remains in the cytoplasm (35, 58). These findings suggest that release of calpain from calpastatin is important for calpain activation. Full-length human calpastatin, which contains domains XL and L and four inhibitory repeats (I–IV), is encoded by class 1 variant and shares homology with the ~145-kDa type II bovine calpastatin. The latter harbors three protein kinase A phosphorylation sites in the XL domain (25). Phosphorylation of calpastatin by protein kinase A *in vivo* increases the amount of membrane-associated calpastatin from 6 to 30% (59). Thus, one would predict that calpastatin isoforms that contain domain XL (encoded by class 1 variants; Fig. 5*B*) are more likely to localize to and inhibit calpain at the plasma membrane compared with the XL-less calpastatin isoform (encoded by class 2 variants), resulting in lower cell migration capacity.

In keeping with the idea that disassociation of calpain from calpastatin at the plasma membrane drives migration, calpastatin was primarily observed in the cytoplasmic perinuclear region of NFI-hypophosphorylated (migratory) U251 MG cells. It is noteworthy that perinuclear localization has been associated with increased calpastatin aggregation, with aggregated calpastatin showing reduced binding to calpain (60). Depletion of NFIs in U251 MG cells (accompanied by reduced class 2 *CAST* variants and increased class 1 *CAST* variants in the case of NFIA depletion) resulted in increased plasma membrane localization of calpastatin. In addition, knockdown of NFIB and NFIX was accompanied by increased nuclear localization of calpastatin (61). Nuclear calpain is believed to promote cell survival through various signaling pathways, including Ku80,

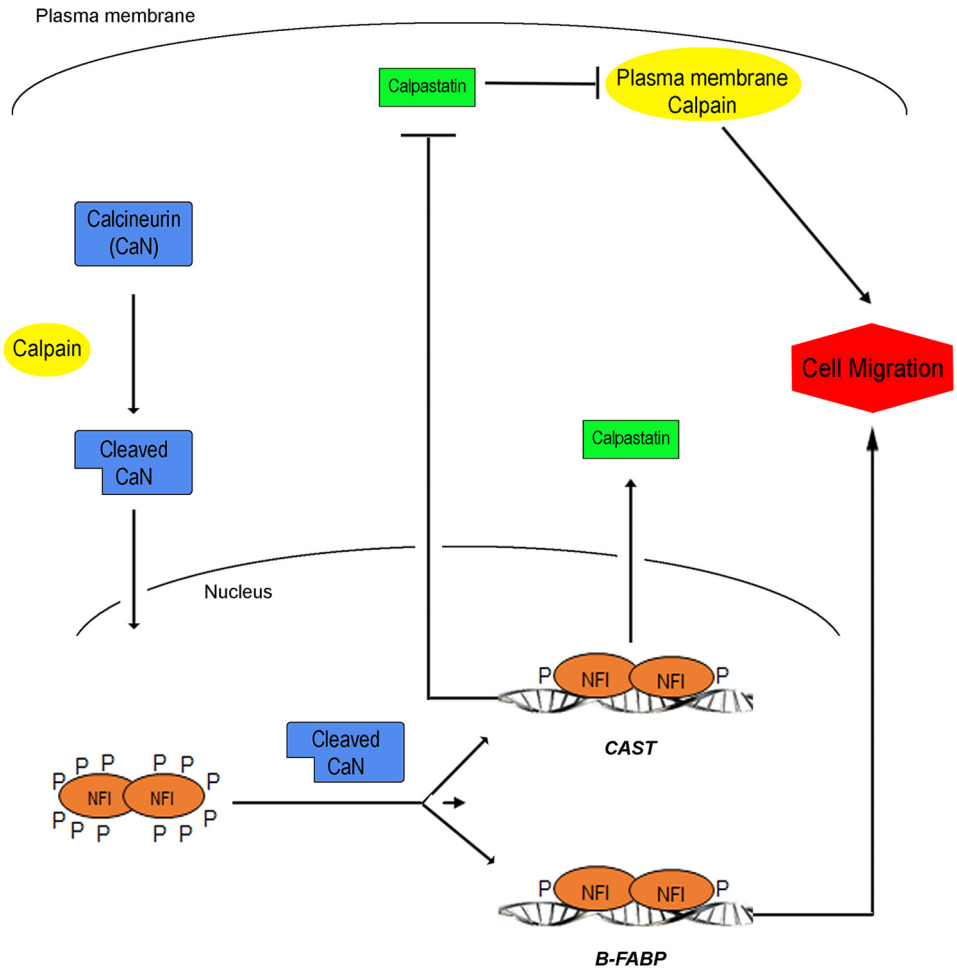

Figure 8. Model of the regulatory cross-talk between the calpain/calpastatin pathway and NFI in MG cells. In the cytoplasm, calcineurin is cleaved and activated by calpain. Activated calcineurin translocates to the nucleus, dephosphorylates, and activates NFI. Hypophosphorylated NFI up-regulates cell migration–promoting *FABP7* as well as *CAST* variants that exclude the XL domain and preferentially localize to the cytoplasm. NFI also negatively affects the expression of plasma membrane–associated full-length calpastatin. As a consequence, calpastatin–calpain interaction at the plasma membrane is reduced, calpain remains active, calpain target effectors are cleaved, and MG cell migration is enhanced.

NF-κB, and phosphatidylinositol 3-kinase/Akt (62–64). As calpastatin is a calpain inhibitor, one may reason that the accumulation of calpastatin in the nucleus of MG cells antagonizes the prosurvival effects mediated by nuclear calpain. Thus, NFIB and NFIX may promote either cell migration or cell death, depending on the ratio of membrane to nuclear calpastatin in MG cells. Such an effect would be consistent with NFIB's paradoxical role, acting either as an oncogene or tumor suppressor, in different types of cancer (65).

We propose that there is regulatory cross-talk between NFIs and the calpastatin/calpain signaling pathway in MG cells that involves the following steps (Fig. 8): (i) calcineurin is cleaved and activated by calpain in the cytoplasm (23); (ii) activated calcineurin translocates to the nucleus and dephosphorylates NFI (21); (iii) hypophosphorylated NFI regulates its target genes (14, 15) including *CAST* through its alternative promoter, which enhances the expression of cytosolic XL-less calpastatin with concomitant suppression of plasma membrane-associated full-length calpastatin; and (iv) in the absence of full-length calpastatin at the plasma membrane, calpain cleaves its cell migration-enhancing effectors, resulting in the increased cell migration associated with NFI-hypophosphorylated MG cells.

In summary, our results indicate that NFIs control the subcellular localization of calpastatin in MG cells through usage of an alternative *CAST* promoter located upstream of exon 4. Binding of hypophosphorylated NFI to *CAST* intron 3 results in increased utilization of the alternative promoter and a higher ratio of class 2 (encoding for XL-less calpastatin isoforms) to class 1 (encoding for full-length calpastatin) *CAST* variants. Depletion of NFIs in NFI-hypophosphorylated MG cells results in accumulation of calpastatin at the plasma membrane. Because calpastatin directly binds and inhibits calpain, regulation of *CAST* variant expression by NFI with accompanying alterations in calpastatin subcellular localization may ultimately control calpain activity. Future work will involve a more in-depth examination of the NFI–calpain signaling pathway, how it affects MG cell migration, and whether it can be exploited to reduce MG infiltration through the inhibition of calpain.

Experimental procedures

Cell lines, constructs, transfections, and treatments

The origins of the MG cell lines used in this study have been described previously (14, 66). Cells were cultured in Dulbecco's

modified Eagle's minimum essential medium supplemented with 10% fetal calf serum, streptomycin (50 μg/ml), and penicillin (50 units/ml). NFI expression constructs, including pCH (empty vector), pCHNFIA, pCHNFIB, pCHNFIC, and pCHNFIX, were a gift from Dr. R. Gronostajski (Case Western Reserve University). Constructs were introduced into MG cells using polyethyleneimine (Polysciences)-mediated transfection with a ratio of 5:1 (μl of polyethyleneimine/μg of DNA). The DNA was removed 18 h after transfection, and cells were harvested 60 h post-transfection.

For CSA treatment, nearly confluent U251 MG cells were treated with either DMSO (negative control) or 1 μM CSA for 1 h at 37 °C. Cells were either harvested for Western blot analysis or fixed for immunofluorescence analysis as described below.

Gel shift assay

Gel shift assays were performed as described previously (15, 67). Probes (C1, C2, and C3) were prepared by annealing complementary oligonucleotides with 5′- and 3′-overhangs, followed by filling in the overhangs with Klenow polymerase and [α-^{32}P]dCTP. Cold competitors were prepared by annealing complementary oligonucleotides in the absence of [α-^{32}P]dCTP. Cold competitors with mutated NFI-binding sites (C2* and C3*) were prepared by replacing the two conserved G residues at positions 3 and 4 with A residues. In addition, C residues at positions 12 and 13 were replaced with A residues in C3* (Fig. 1). NFI and AP2 consensus competitor oligonucleotides were synthesized by annealing 5′-ATTTTGGCTTGAAGCCAATATG-3′ and 5′-CATATTGGCTTCAAGCCAAAAT-3′ (NFI consensus binding site is underlined) and 5′-GATCGAACTGACCGCCCGCGGCCCGT-3′ and 5′-ACGGGCCGCGGGCGGTCAGTTCGATC-3′ (AP2 consensus binding site underlined). U87 and U251 MG cells were transiently transfected with 7 μg of each of the HA-tagged NFI expression constructs (pCH, pCHNFIA, pCHNFIB, pCHNFIC, and pCHNFIX) or siRNA targeting NFIC as described below. Nuclear extracts were prepared using NE-PER® nuclear and cytoplasmic extraction reagents (Thermo Fisher Scientific). Four μg of nuclear extracts prepared from NFI or pCH-transfected cells were preincubated in binding buffer (20 mM Hepes, pH 7.9, 1 mM spermidine, 10 mM DTT, 20 mM KCl, 0.1% Nonidet P-40, 10% glycerol) in the presence of 1 μg of poly(dI-dC) for 10 min at room temperature. Where indicated, a 100-fold molar excess of unlabeled competitor oligonucleotide was added to the reaction. For supershift experiments, 0.5 μg of anti-AP2 (Santa Cruz Biotechnology, Inc.), anti-HA (Roche Applied Science), pan-specific anti-NFI (obtained from Dr. Naoko Tanese), anti-NFIA (custom polyclonal antibody, antigen CPDTKPPTTSTEGGA; GenScript), anti-NFIB (custom polyclonal antibody, antigen CSGSPSHNDPAKNPP; GenScript), anti-NFIC (custom polyclonal antibody, antigen CDQEDSKPITLDTTD; GenScript), or anti-NFIX (custom polyclonal antibody, antigen CDGSGQATGQHSQRQ; GenScript) antibodies were included during the preincubation stage. Next, radiolabeled oligonucleotides were added, followed by an incubation period of 20 min at room temperature. Reactions were then electrophoresed in a 6% nondenaturing polyacrylamide gel in 0.5× TBE (Tris-borate EDTA). The gels were dried and exposed to X-ray film.

Knockdown of endogenous NFIs and CAST

U87, T98, and/or U251 MG cells were transfected with the following NFI-targeting Stealth® siRNAs: control scrambled siRNA (catalog nos. 12935-200 and 12935-300 (Invitrogen)), NM_005595_stealth_919 (5′-GAAAGUUCUUCAUACUACAGCAUGA-3′ of NFIA), NM_005596_stealth_1020 (5′-AAGCCACAAUGAUCCUGCCAAGAAU-3′ of NFIB), NM_005597_stealth_1045 (5′-CAGAGAUGGACAAGUCACCAUUCAA-3′ of NFIC), NM_002501_stealth_752 (5′-GAGAGUAUCACAGACUCCUGUUGCA-3′ of NFIX), NM_001042440.3_stealth_486 (5′-UCCUCUGGUGCAACCAGCAAGUCUU-3′ of *CAST*), and NM_00190442.1_stealth_1264 (5′-ACAAUCCCAUCUGAGUACAGAUUAA-3′ of *CAST*). Cells were transfected with a 10 nM concentration of each siRNA using the RNAiMAX Lipofectamine reagent (Invitrogen) according to the manufacturer's protocol. After 48 h, cells were split 1 in 6 and transfected with another round of siRNA. Cells were harvested 60 h after the second transfection.

RT-qPCR

Total RNA was isolated from transfected cells using the TRIzol® reagent (Thermo Fisher Scientific). First-strand cDNA was synthesized using Superscript II® reverse transcriptase (Invitrogen). For RT-PCR, cDNAs were amplified using primers to the different NFIs or β-actin, which served as the loading control (see Table 1 for a list of primers). For qPCR, cDNAs were amplified using primer pairs targeting specific regions of the *CAST* gene and the BrightGreen® qPCR master mix (ABM Scientific). qPCR results were normalized to *GAPDH*. Relative -fold change was generated by normalizing each treatment to the respective scrambled siRNA control.

ChIP

ChIP was carried out as previously described (68). Briefly, MG cells were cross-linked with 1% formaldehyde for 20 min at room temperature. Cross-linking was terminated using glycine to a final concentration of 0.125 M. Cells were then collected in 1× PBS supplemented with 0.5 mM phenylmethylsulfonyl fluoride, washed, and resuspended in lysis buffer (44 mM Tris-HCl, pH 8.0, 10 mM EDTA, 1% SDS, 1× Complete® protease inhibitors (Roche Applied Science)). Cells were sonicated twice at 4 °C for 10 cycles (1 min/cycle, 30 s power on and 30 s power off) with output level set to high (Bioruptor 300® ultrasonic homogenizer, Diagenode). Next, lysates were precleared twice (constant rotation at 4 °C for 1 h) with protein G-Sepharose Fast Flow beads (Sigma Aldrich) and SDS diluted to 0.1%. Either 2 μg of rabbit (for NFI) or mouse (for RNA polymerase II) IgG (negative control), 2 μg of a pan-specific anti-NFI antibody (obtained from Dr. Naoko Tanese), or 2 μg of anti-RNA polymerase II antibody (Abcam) were incubated with lysates at 4 °C overnight with constant rotation. Protein G-Sepharose beads were added to reactions and incubated at 4 °C for 2 h. Beads were washed in buffers of increasing stringency (140 mM NaCl to 500 mM NaCl to 250 mM LiCl). Protein–DNA complexes were eluted in 0.1 M $NaHCO_3$, 5 mM NaCl, 1% SDS and incubated at 65 °C overnight to reverse cross-links. DNA was purified by phenol-chloroform extraction, followed by ethanol precipitation. *CAST* NFI-binding regions (C2 and C3) as well as

GAPDH promoter (negative control) were amplified (Table 1) using the following parameters: 95 °C for 3 min; 35 cycles at 95 °C for 30 s, 60 °C for 30 s, and 72 °C for 30 s; 72 °C for 7 min. Amplified DNA was resolved in 1.5% agarose gels and visualized using ethidium bromide. For quantitative analysis, chromatin-immunoprecipitated DNA was amplified by qPCR using the primers listed in Table 1. Results are presented as relative -fold change compared with IgG negative control.

RLM RACE

Total RNA was isolated from T98 and U251 MG cells as described above. *CAST* cDNA was generated using the FirstChoice® RLM RACE kit (Ambion) according to the manufacturer's protocol. Briefly, 5 μg of total RNA was digested with calf intestinal alkaline phosphatase to remove the 5′-phosphate group from non-mRNA molecules as well as degraded mRNAs. Intact mRNA is capped and remains uncleaved by calf intestinal alkaline phosphatase. The 5′-cap was then removed with tobacco acid pyrophosphatase, yielding a 5′-monophosphate to which an RNA adapter with known sequence was ligated using T4 RNA ligase. *CAST*-specific primer (Table 1) was used to reverse-transcribe RNA with Moloney murine leukemia virus reverse transcriptase. cDNAs were PCR-amplified using nested primer pairs (Table 1). The DNA was electrophoresed in a 3% MetaPhor agarose (FMC Bioproducts, Rockland, ME) gel, excised, purified (Monarch DNA extraction kit, New England Biolabs), and sequenced (BigDye Terminator® version 3.1 cycle sequencing kit, Thermo Fisher Scientific).

Luciferase reporter gene assay

The following reporter gene constructs were generated using the pGL3 luciferase vector (Promega) with the SV40 promoter element removed: (i) empty vector control (CNT), (ii) −1990 to +50 bp of the *CAST* promoter linked to the luciferase gene, with +1 denoting the first nucleotide of exon 1 (designated CP for canonical promoter region), and (iii) −4026 to +20 bp relative to exon 4, with +1 denoting the first nucleotide exon 4 (designated ALT for NFI-bound alternative promoter). Site-directed mutagenized ALT-C2*, ALT-C3*, and ALT-C2*3* constructs were generated using the QuikChange® site-directed mutagenesis kit (Agilent Technologies), as indicated in Fig. 1. Cells were transfected with luciferase reporter constructs using JetPrime® transfection reagent (VWR) according to the manufacturer's instructions. Transfected cells were lysed directly on the plate using Promega's Cell Culture Lysis Buffer for 20 min at room temperature. Equal amounts of luciferase substrate were added to 20 μl of protein lysates, and light emitted from the bioluminescent conversion of D-luciferin to oxyluciferin was measured with the FLUOstar OPTIMA (BMG LABTECH) microplate reader. Relative light units/μg were obtained by dividing the amount of light emitted from each sample by their respective protein concentration (measured using the Bradford reagent). Relative -fold change was calculated by normalizing the relative light units/μg of each promoter construct against the value for the empty vector control.

Western blot analysis

Nuclear extracts were prepared using the NE-PER® nuclear and cytoplasmic extraction reagents (Thermo Fisher Scientific). Whole-cell lysates were prepared by syringing cells 15–20 times (23-gauge needles) at 4 °C in lysis buffer (50 mM Tris-HCl, pH 7.5, 1% sodium deoxycholate, 1% Triton X-100, 150 mM NaCl, 50 mM sodium fluoride, 1 mM sodium orthovanadate, 10 mM EDTA, 0.1% SDS, 1× Complete protease inhibitor (Roche Applied Science), and 1× PhosSTOP phosphatase inhibitor (Roche Applied Science)). Proteins were resolved in SDS-polyacrylamide gels and electroblotted onto polyvinylidene fluoride or nitrocellulose membranes. Blots were immunostained with rabbit pan-specific anti-calpastatin antibody (1:10,000; Santa Cruz Biotechnology), mouse anti-β-actin antibody (1:100,000; Sigma-Aldrich), mouse anti-HA antibody (1:5000; Roche Applied Science), mouse pan-specific anti-NFI antibody (1:1000; Santa Cruz Biotechnology), or α-tubulin (1:50,000; Hybridoma Bank) followed by detection with horseradish peroxidase–conjugated secondary antibody (Jackson ImmunoResearch Biotech) using the Immobilon® Western chemiluminescent horseradish peroxidase substrate (EMD Millipore).

Immunofluorescence analysis

Cells were transfected with the indicated siRNAs and plated onto glass coverslips 48 h after transfection. Twenty-four h later, cells were fixed with 4% paraformaldehyde for 10 min and permeabilized with 0.25% Triton X-100 for 4 min, followed by blocking with 3% BSA for 45 min at room temperature. Cells were immunostained with rabbit anti-calpastatin (1:100; Santa Cruz Biotechnology) primary antibody, followed by Alexa 488–conjugated donkey anti-rabbit antibody (1:400; Life Technologies, Inc.). To reduce background signal, the coverslips were washed with 0.01% Tween 20 in PBS for 5 min followed by two 5-min washes with PBS alone after each antibody incubation. Coverslips were mounted onto microscope slides with polyvinyl alcohol–based medium containing 1 μg/ml 4′,6-diamidino-2-phenylindole (Calbiochem). Images were acquired with a ×40/1.3 numerical aperture oil immersion lens on a Zeiss LSM 710 confocal microscope using the ZEN software (Zeiss).

Author contributions—T. M. V., R. B., and R. G. conceptualization; T. M. V. and R. G. resources; T. M. V., R. B., and M. B. data curation; T. M. V., R. B., M. B., E. A. M., H.-Y. P., and R. G. formal analysis; T. M. V. and R. G. supervision; T. M. V. and R. G. funding acquisition; T. M. V., R. B., E. A. M., and H.-Y. P. validation; T. M. V., R. B., M. B., and R. G. investigation; T. M. V., R. B., and M. B. visualization; T. M. V., R. B., M. B., E. A. M., H.-Y. P., and R. G. methodology; T. M. V. and R. B. writing-original draft; T. M. V. and R. G. project administration; T. M. V., R. B., M. B., E. A. M., H.-Y. P., and R. G. writing-review and editing.

Acknowledgments—We thank Dr. R. Gronostajski (Case Western Reserve University) and Dr. Naoko Tanese (New York University Medical Center) for the NFI expression constructs and anti-NFI antibody, respectively. We are grateful to Xuejun Sun, Gerry Barron, and the Cross Cancer Institute Cell Imaging Facility for support with imaging MG cells.

References

1. Omuro, A., and DeAngelis, L. M. (2013) Glioblastoma and other malignant gliomas: a clinical review. *JAMA* **310,** 1842–1850 CrossRef Medline
2. Ostrom, Q. T., Gittleman, H., Fulop, J., Liu, M., Blanda, R., Kromer, C., Wolinsky, Y., Kruchko, C., and Barnholtz-Sloan, J. S. (2015) CBTRUS Statistical Report: primary brain and central nervous system tumors diagnosed in the United States in 2008–2012. *Neuro Oncol.* **17,** iv1–iv62 CrossRef Medline
3. Mason, W. P., Maestro, R. D., Eisenstat, D., Forsyth, P., Fulton, D., Laperrière, N., Macdonald, D., Perry, J., Thiessen, B., Canadian GBM Recommendations Committee (2007) Canadian recommendations for the treatment of glioblastoma multiforme. *Curr. Oncol.* **14,** 110–117 CrossRef Medline
4. Claes, A., Idema, A. J., and Wesseling, P. (2007) Diffuse glioma growth: a guerilla war. *Acta Neuropathol.* **114,** 443–458 CrossRef Medline
5. de Groot, J. F., Fuller, G., Kumar, A. J., Piao, Y., Eterovic, K., Ji, Y., and Conrad, C. A. (2010) Tumor invasion after treatment of glioblastoma with bevacizumab: radiographic and pathologic correlation in humans and mice. *Neuro Oncol.* **12,** 233–242 CrossRef Medline
6. Kallenberg, K., Goldmann, T., Menke, J., Strik, H., Bock, H. C., Stockhammer, F., Buhk, J. H., Frahm, J., Dechent, P., and Knauth, M. (2013) Glioma infiltration of the corpus callosum: early signs detected by DTI. *J. Neurooncol.* **112,** 217–222 CrossRef Medline
7. Norden, A. D., Young, G. S., Setayesh, K., Muzikansky, A., Klufas, R., Ross, G. L., Ciampa, A. S., Ebbeling, L. G., Levy, B., Drappatz, J., Kesari, S., and Wen, P. Y. (2008) Bevacizumab for recurrent malignant gliomas: efficacy, toxicity, and patterns of recurrence. *Neurology* **70,** 779–787 CrossRef Medline
8. Ogura, K., Mizowaki, T., Arakawa, Y., Ogura, M., Sakanaka, K., Miyamoto, S., and Hiraoka, M. (2013) Initial and cumulative recurrence patterns of glioblastoma after temozolomide-based chemoradiotherapy and salvage treatment: a retrospective cohort study in a single institution. *Radiat. Oncol.* **8,** 97 CrossRef Medline
9. Shankar, A., Kumar, S., Iskander, A. S., Varma, N. R., Janic, B., deCarvalho, A., Mikkelsen, T., Frank, J. A., Ali, M. M., Knight, R. A., Brown, S., and Arbab, A. S. (2014) Subcurative radiation significantly increases cell proliferation, invasion, and migration of primary glioblastoma multiforme *in vivo*. *Chin. J. Cancer* **33,** 148–158 CrossRef Medline
10. Mita, R., Coles, J. E., Glubrecht, D. D., Sung, R., Sun, X., and Godbout, R. (2007) B-FABP-expressing radial glial cells: the malignant glioma cell of origin? *Neoplasia* **9,** 734–744 CrossRef Medline
11. Kaloshi, G., Mokhtari, K., Carpentier, C., Taillibert, S., Lejeune, J., Marie, Y., Delattre, J. Y., Godbout, R., and Sanson, M. (2007) FABP7 expression in glioblastomas: relation to prognosis, invasion and EGFR status. *J. Neurooncol.* **84,** 245–248 CrossRef Medline
12. Liang, Y., Diehn, M., Watson, N., Bollen, A. W., Aldape, K. D., Nicholas, M. K., Lamborn, K. R., Berger, M. S., Botstein, D., Brown, P. O., and Israel, M. A. (2005) Gene expression profiling reveals molecularly and clinically distinct subtypes of glioblastoma multiforme. *Proc. Natl. Acad. Sci. U.S.A.* **102,** 5814–5819 CrossRef Medline
13. De Rosa, A., Pellegatta, S., Rossi, M., Tunici, P., Magnoni, L., Speranza, M. C., Malusa, F., Miragliotta, V., Mori, E., Finocchiaro, G., and Bakker, A. (2012) A radial glia gene marker, fatty acid binding protein 7 (FABP7), is involved in proliferation and invasion of glioblastoma cells. *PLoS One* **7,** e52113 CrossRef Medline
14. Brun, M., Coles, J. E., Monckton, E. A., Glubrecht, D. D., Bisgrove, D., and Godbout, R. (2009) Nuclear factor I regulates brain fatty acid-binding protein and glial fibrillary acidic protein gene expression in malignant glioma cell lines. *J. Mol. Biol.* **391,** 282–300 CrossRef Medline
15. Bisgrove, D. A., Monckton, E. A., Packer, M., and Godbout, R. (2000) Regulation of brain fatty acid-binding protein expression by differential phosphorylation of nuclear factor I in malignant glioma cell lines. *J. Biol. Chem.* **275,** 30668–30676 CrossRef Medline
16. Kruse, U., and Sippel, A. E. (1994) Transcription factor nuclear factor I proteins form stable homo- and heterodimers. *FEBS Lett.* **348,** 46–50 CrossRef Medline
17. Roulet, E., Bucher, P., Schneider, R., Wingender, E., Dusserre, Y., Werner, T., and Mermod, N. (2000) Experimental analysis and computer prediction of CTF/NFI transcription factor DNA binding sites. *J. Mol. Biol.* **297,** 833–848 CrossRef Medline
18. Gronostajski, R. M. (1986) Analysis of nuclear factor I binding to DNA using degenerate oligonucleotides. *Nucleic Acids Res.* **14,** 9117–9132 CrossRef Medline
19. Gronostajski, R. M. (2000) Roles of the NFI/CTF gene family in transcription and development. *Gene* **249,** 31–45 CrossRef Medline
20. Heng, Y. H., Barry, G., Richards, L. J., and Piper, M. (2012) Nuclear factor I genes regulate neuronal migration. *Neurosignals* **20,** 159–167 CrossRef Medline
21. Brun, M., Glubrecht, D. D., Baksh, S., and Godbout, R. (2013) Calcineurin regulates nuclear factor I dephosphorylation and activity in malignant glioma cell lines. *J. Biol. Chem.* **288,** 24104–24115 CrossRef Medline
22. Kim, M. J., Jo, D. G., Hong, G. S., Kim, B. J., Lai, M., Cho, D. H., Kim, K. W., Bandyopadhyay, A., Hong, Y. M., Kim, D. H., Cho, C., Liu, J. O., Snyder, S. H., and Jung, Y. K. (2002) Calpain-dependent cleavage of cain/cabin1 activates calcineurin to mediate calcium-triggered cell death. *Proc. Natl. Acad. Sci. U.S.A.* **99,** 9870–9875 CrossRef Medline
23. Wu, H. Y., Tomizawa, K., Oda, Y., Wei, F. Y., Lu, Y. F., Matsushita, M., Li, S. T., Moriwaki, A., and Matsui, H. (2004) Critical role of calpain-mediated cleavage of calcineurin in excitotoxic neurodegeneration. *J. Biol. Chem.* **279,** 4929–4940 CrossRef Medline
24. Wendt, A., Thompson, V. F., and Goll, D. E. (2004) Interaction of calpastatin with calpain: a review. *Biol. Chem.* **385,** 465–472 Medline
25. Cong, M., Thompson, V. F., Goll, D. E., and Antin, P. B. (1998) The bovine calpastatin gene promoter and a new N-terminal region of the protein are targets for cAMP-dependent protein kinase activity. *J. Biol. Chem.* **273,** 660–666 CrossRef Medline
26. Lee, W. J., Ma, H., Takano, E., Yang, H. Q., Hatanaka, M., and Maki, M. (1992) Molecular diversity in amino-terminal domains of human calpastatin by exon skipping. *J. Biol. Chem.* **267,** 8437–8442 Medline
27. Parr, T., Sensky, P. L., Bardsley, R. G., and Buttery, P. J. (2001) Calpastatin expression in porcine cardiac and skeletal muscle and partial gene structure. *Arch. Biochem. Biophys.* **395,** 1–13 CrossRef Medline
28. Emori, Y., Kawasaki, H., Imajoh, S., Minami, Y., and Suzuki, K. (1988) All four repeating domains of the endogenous inhibitor for calcium-dependent protease independently retain inhibitory activity: expression of the cDNA fragments in *Escherichia coli*. *J. Biol. Chem.* **263,** 2364–2370 Medline
29. De Tullio, R., Averna, M., Stifanese, R., Parr, T., Bardsley, R. G., Pontremoli, S., and Melloni, E. (2007) Multiple rat brain calpastatin forms are produced by distinct starting points and alternative splicing of the N-terminal exons. *Arch. Biochem. Biophys.* **465,** 148–156 CrossRef Medline
30. Takano, J., Watanabe, M., Hitomi, K., and Maki, M. (2000) Four types of calpastatin isoforms with distinct amino-terminal sequences are specified by alternative first exons and differentially expressed in mouse tissues. *J. Biochem.* **128,** 83–92 CrossRef Medline
31. Lane, R. D., Allan, D. M., and Mellgren, R. L. (1992) A comparison of the intracellular distribution of μ-calpain, m-calpain, and calpastatin in proliferating human A431 cells. *Exp. Cell Res.* **203,** 5–16 CrossRef Medline
32. Goll, D. E., Thompson, V. F., Li, H., Wei, W., and Cong, J. (2003) The calpain system. *Physiol. Rev.* **83,** 731–801 CrossRef Medline
33. Averna, M., de Tullio, R., Passalacqua, M., Salamino, F., Pontremoli, S., and Melloni, E. (2001) Changes in intracellular calpastatin localization are mediated by reversible phosphorylation. *Biochem. J.* **354,** 25–30 CrossRef Medline
34. Perrin, B. J., and Huttenlocher, A. (2002) Calpain. *Int. J. Biochem. Cell Biol.* **34,** 722–725 CrossRef Medline
35. Gil-Parrado, S., Popp, O., Knoch, T. A., Zahler, S., Bestvater, F., Felgentträger, M., Holloschi, A., Fernández-Montalvan, A., Auerswald, E. A., Fritz, H., Fuentes-Prior, P., Machleidt, W., and Spiess, E. (2003) Subcellular localization and in vivo subunit interactions of ubiquitous μ-calpain. *J. Biol. Chem.* **278,** 16336–16346 CrossRef Medline
36. Brun, M., Jain, S., Monckton, E. A., and Godbout, R. (2018) Nuclear Factor I Represses the Notch Effector HEY1 in Glioblastoma. *Neoplasia* **20,** 1023–1037 CrossRef Medline

37. Komarnitsky, P., Cho, E. J., and Buratowski, S. (2000) Different phosphorylated forms of RNA polymerase II and associated mRNA processing factors during transcription. *Genes Dev.* **14,** 2452–2460 CrossRef Medline
38. Leloup, L., Shao, H., Bae, Y. H., Deasy, B., Stolz, D., Roy, P., and Wells, A. (2010) m-Calpain activation is regulated by its membrane localization and by its binding to phosphatidylinositol 4,5-bisphosphate. *J. Biol. Chem.* **285,** 33549–33566 CrossRef Medline
39. Shao, H., Chou, J., Baty, C. J., Burke, N. A., Watkins, S. C., Stolz, D. B., and Wells, A. (2006) Spatial localization of m-calpain to the plasma membrane by phosphoinositide biphosphate binding during epidermal growth factor receptor-mediated activation. *Mol. Cell. Biol.* **26,** 5481–5496 CrossRef Medline
40. Deneen, B., Ho, R., Lukaszewicz, A., Hochstim, C. J., Gronostajski, R. M., and Anderson, D. J. (2006) The transcription factor NFIA controls the onset of gliogenesis in the developing spinal cord. *Neuron* **52,** 953–968 CrossRef Medline
41. Namihira, M., Kohyama, J., Semi, K., Sanosaka, T., Deneen, B., Taga, T., and Nakashima, K. (2009) Committed neuronal precursors confer astrocytic potential on residual neural precursor cells. *Dev. Cell* **16,** 245–255 CrossRef Medline
42. Mason, S., Piper, M., Gronostajski, R. M., and Richards, L. J. (2009) Nuclear factor one transcription factors in CNS development. *Mol. Neurobiol.* **39,** 10–23 CrossRef Medline
43. Kang, P., Lee, H. K., Glasgow, S. M., Finley, M., Donti, T., Gaber, Z. B., Graham, B. H., Foster, A. E., Novitch, B. G., Gronostajski, R. M., and Deneen, B. (2012) Sox9 and NFIA coordinate a transcriptional regulatory cascade during the initiation of gliogenesis. *Neuron* **74,** 79–94 CrossRef Medline
44. Mita, R., Beaulieu, M. J., Field, C., and Godbout, R. (2010) Brain fatty acid-binding protein and ω-3/ω-6 fatty acids: mechanistic insight into malignant glioma cell migration. *J. Biol. Chem.* **285,** 37005–37015 CrossRef Medline
45. Alevizopoulos, A., Dusserre, Y., Rüegg, U., and Mermod, N. (1997) Regulation of the transforming growth factor β-responsive transcription factor CTF-1 by calcineurin and calcium/calmodulin-dependent protein kinase IV. *J. Biol. Chem.* **272,** 23597–23605 CrossRef Medline
46. Wu, H. Y., Tomizawa, K., and Matsui, H. (2007) Calpain-calcineurin signaling in the pathogenesis of calcium-dependent disorder. *Acta Med. Okayama* **61,** 123–137 Medline
47. Ding, F., Li, X., Li, B., Guo, J., Zhang, Y., and Ding, J. (2016) Calpain-mediated cleavage of calcineurin in puromycin aminonucleoside-induced podocyte injury. *PLoS One* **11,** e0155504 CrossRef Medline
48. Santos, D. M., Xavier, J. M., Morgado, A. L., Solá, S., and Rodrigues, C. M. (2012) Distinct regulatory functions of calpain 1 and 2 during neural stem cell self-renewal and differentiation. *PLoS One* **7,** e33468 CrossRef Medline
49. Chan, K. T., Bennin, D. A., and Huttenlocher, A. (2010) Regulation of adhesion dynamics by calpain-mediated proteolysis of focal adhesion kinase (FAK). *J. Biol. Chem.* **285,** 11418–11426 CrossRef Medline
50. Lebart, M. C., and Benyamin, Y. (2006) Calpain involvement in the remodeling of cytoskeletal anchorage complexes. *FEBS J.* **273,** 3415–3426 CrossRef Medline
51. Cortesio, C. L., Chan, K. T., Perrin, B. J., Burton, N. O., Zhang, S., Zhang, Z. Y., and Huttenlocher, A. (2008) Calpain 2 and PTP1B function in a novel pathway with Src to regulate invadopodia dynamics and breast cancer cell invasion. *J. Cell Biol.* **180,** 957–971 CrossRef Medline
52. Franco, S., Perrin, B., and Huttenlocher, A. (2004) Isoform specific function of calpain 2 in regulating membrane protrusion. *Exp. Cell Res.* **299,** 179–187 CrossRef Medline
53. Lal, S., La Du, J., Tanguay, R. L., and Greenwood, J. A. (2012) Calpain 2 is required for the invasion of glioblastoma cells in the zebrafish brain microenvironment. *J. Neurosci. Res.* **90,** 769–781 CrossRef Medline
54. Tangmansakulchai, K., Abubakar, Z., Kitiyanant, N., Suwanjang, W., Leepiyasakulchai, C., Govitrapong, P., and Chetsawang, B. (2016) Calpastatin overexpression reduces oxidative stress-induced mitochondrial impairment and cell death in human neuroblastoma SH-SY5Y cells by decreasing calpain and calcineurin activation, induction of mitochondrial fission and destruction of mitochondrial fusion. *Mitochondrion* **30,** 151–161 CrossRef Medline
55. Schoch, K. M., Evans, H. N., Brelsfoard, J. M., Madathil, S. K., Takano, J., Saido, T. C., and Saatman, K. E. (2012) Calpastatin overexpression limits calpain-mediated proteolysis and behavioral deficits following traumatic brain injury. *Exp. Neurol.* **236,** 371–382 CrossRef Medline
56. Nilsson, E., Alafuzoff, I., Blennow, K., Blomgren, K., Hall, C. M., Janson, I., Karlsson, I., Wallin, A., Gottfries, C. G., and Karlsson, J. O. (1990) Calpain and calpastatin in normal and Alzheimer-degenerated human brain tissue. *Neurobiol. Aging* **11,** 425–431 CrossRef Medline
57. Gronostajski, R. M. (1987) Site-specific DNA binding of nuclear factor I: effect of the spacer region. *Nucleic Acids Res.* **15,** 5545–5559 CrossRef Medline
58. Stifanese, R., Averna, M., De Tullio, R., Pedrazzi, M., Beccaria, F., Salamino, F., Milanese, M., Bonanno, G., Pontremoli, S., and Melloni, E. (2010) Adaptive modifications in the calpain/calpastatin system in brain cells after persistent alteration in Ca^{2+} homeostasis. *J. Biol. Chem.* **285,** 631–643 CrossRef Medline
59. Adachi, Y., Takano, E., Murachi, T., and Hatanaka, M. (1988) Distribution and expression of calpastatin in human hematopoietic system cells. *Biol. Chem. Hoppe Seyler* **369,** 223–227 Medline
60. Averna, M., De Tullio, R., Capini, P., Salamino, F., Pontremoli, S., and Melloni, E. (2003) Changes in calpastatin localization and expression during calpain activation: a new mechanism for the regulation of intracellular Ca^{2+}-dependent proteolysis. *Cell Mol. Life Sci.* **60,** 2669–2678 CrossRef Medline
61. Perrin, B. J., Amann, K. J., and Huttenlocher, A. (2006) Proteolysis of cortactin by calpain regulates membrane protrusion during cell migration. *Mol. Biol. Cell* **17,** 239–250 CrossRef Medline
62. Baek, K. H., Yu, H. V., Kim, E., Na, Y., and Kwon, Y. (2016) Calcium influx-mediated translocation of m-calpain induces Ku80 cleavage and enhances the Ku80-related DNA repair pathway. *Oncotarget* **7,** 30831–30844 Medline
63. Baghdiguian, S., Martin, M., Richard, I., Pons, F., Astier, C., Bourg, N., Hay, R. T., Chemaly, R., Halaby, G., Loiselet, J., Anderson, L. V., Lopez de Munain, A., Fardeau, M., Mangeat, P., Beckmann, J. S., and Lefranc, G. (1999) Calpain 3 deficiency is associated with myonuclear apoptosis and profound perturbation of the IκB α/NF-κB pathway in limb-girdle muscular dystrophy type 2A. *Nat. Med.* **5,** 503–511 CrossRef Medline
64. Tremper-Wells, B., and Vallano, M. L. (2005) Nuclear calpain regulates Ca^{2+}-dependent signaling via proteolysis of nuclear Ca^{2+}/calmodulin-dependent protein kinase type IV in cultured neurons. *J. Biol. Chem.* **280,** 2165–2175 CrossRef Medline
65. Becker-Santos, D. D., Lonergan, K. M., Gronostajski, R. M., and Lam, W. L. (2017) Nuclear factor I/B: a master regulator of cell differentiation with paradoxical roles in cancer. *EBioMedicine* **22,** 2–9 CrossRef Medline
66. Godbout, R., Bisgrove, D. A., Shkolny, D., and Day, R. S., 3rd (1998) Correlation of B-FABP and GFAP expression in malignant glioma. *Oncogene* **16,** 1955–1962 CrossRef Medline
67. O'Brien, R. M., Noisin, E. L., Suwanichkul, A., Yamasaki, T., Lucas, P. C., Wang, J. C., Powell, D. R., and Granner, D. K. (1995) Hepatic nuclear factor 3- and hormone-regulated expression of the phosphoenolpyruvate carboxykinase and insulin-like growth factor-binding protein 1 genes. *Mol. Cell. Biol.* **15,** 1747–1758 CrossRef Medline
68. Pillai, S., Dasgupta, P., and Chellappan, S. P. (2009) Chromatin immunoprecipitation assays: analyzing transcription factor binding and histone modifications *in vivo*. *Methods Mol. Biol.* **523,** 323–339 CrossRef Medline

Effects of nuclear factor I phosphorylation on calpastatin (*CAST*) gene variant expression and subcellular distribution in malignant glioma cells

The Minh Vo, Rebecca Burchett, Miranda Brun, Elizabeth A. Monckton, Ho-Yin Poon and Roseline Godbout

J. Biol. Chem. 2019, 294:1173-1188.
doi: 10.1074/jbc.RA118.004787 originally published online November 30, 2018